17

The Chemistry of the Troposphere

Chapters 13–16 focused on the processes responsible for production and removal of O_3 in the stratosphere; in a larger sense they concerned the response of the stratosphere to absorption of ultraviolet solar radiation and the sequence of reactions triggered by photodissociation of O_2 at wavelengths less than about 240 nm. We saw that dissociation of O_2 results in the production of O and subsequently of O_3. The presence of O_3 extends the spectral range for absorption of ultraviolet solar radiation by almost 70 nm (to about 310 nm) and plays a critical role in shielding life at Earth's surface from potentially lethal doses of ultraviolet (UV-B) radiation. The abundance of O_3 reflects an overall balance between the rate at which odd oxygen (mainly $O + O_3$: see definition in Section 13.1) is formed by photodissociation of O_2 and the rate at which it is removed, primarily by reactions catalyzed by trace abundances of nitrogen, hydrogen, chlorine, and bromine radicals. But the balance is not entirely local; odd oxygen formed in one region may be transported over large distances by atmospheric winds and eventually removed far from its point of origin. Transport is particularly important at lower altitudes and at higher latitudes, where the lifetime of odd oxygen is long. A small fraction (about 1%) of odd oxygen formed in the stratosphere makes its way to the troposphere. As we shall see, the supply of O_3 from the stratosphere plays a critical catalytic role in the chemistry of the troposphere.

The troposphere is in a real sense an extension of the biosphere. A large variety of reduced gases is produced and released to the atmosphere as by-products of the metabolism of bacteria, plants, and animals. Methane is formed by bacteria breaking down plant material under anaerobic (low-oxygen) conditions in swamps and rice fields and in the stomachs of cud-chewing ruminants, such as cattle and sheep. Bacteria are also responsible for production of important quantities of nitrogen oxides and hydrogen sulfide, from soils and swamps, respectively. Land-based plants emit a variety of hydrocarbons: notably isoprene and various terpenes. Marine phytoplankton contribute a significant source of dimethylsulfide. Adding to the mix of chemically reduced species is a wide range of gases, including carbon monoxide, methane, and nitric oxide, emitted as by-products of the burning of vegetation (fires naturally initiated by lightning, as well as fires set for various purposes by humans) and the combustion of fossil fuels. Additional production of reduced species is associated with industry and with disposal and decomposition of human and animal wastes. In the absence of mechanisms for removal and recycling of the waste products of life—the waste gases of the biosphere and industry—the composition of the atmosphere would radically change and we would literally choke on our own exhaust; this chapter is concerned with elaboration of the processes regulating the self-cleansing properties of the atmosphere.

In our discussion of tropospheric chemistry, we will be especially interested in processes that contribute to the recycling in the atmosphere of

the life-essential elements C, N, and S. Specifically, we are concerned with the fate of these elements as they are emitted in reduced, or partially reduced form (see Section 3.2 for a discussion of the distinction between reduced and oxidized states of elements in specific compounds and for the recipe used to measure the degree of oxidation: the oxidation number) by the biosphere or by industry. The breakdown, transformation, and ultimate removal of reduced forms of C, N, and S involve a series of reactions in which the elements are sequentially converted to higher states of oxidation. As we shall see, depending on circumstances, these reactions can be responsible for significant production or, under some circumstances, important loss of O_3.

Carbon in living tissue (denoted symbolically by CH_2O: see Section 11.1) is characterized by an oxidation number of 0. The oxidation states for carbon in CH_4 and CO are −4 and +2, respectively.[1] Reduced forms of carbon are converted in the atmosphere to the fully oxidized state, CO_2 (carbon oxidation state +4), which is subsequently taken up by plants, completing the cycle summarized by reactions (11.1) and (11.2).

Nitrogen in NO has an oxidation number of +2. Nitrogen in nitric acid (HNO_3), the form in which N is typically removed from the atmosphere, has an oxidation number of +5. Similarly, sulfur in hydrogen sulfide, H_2S, or dimethylsulfide, $(CH_3)_2S$, has an oxidation number of −2. Sulfur is removed from the atmosphere mainly in the oxidation state +6 as sulfuric acid (H_2SO_4). The fully oxidized forms of nitrogen and sulfur are soluble and are readily scavenged from the atmosphere by rain and snow and by deposition on moist surfaces (plant leaves, for example). They are subsequently taken up and reduced by plants, completing the cycle. A steady state is established for N and S, as it is for C: the release of N and S originally contained in plant material into the atmosphere is balanced by oxidation in the atmosphere, followed by either dry or wet deposition (for definition of these terms, see Endnote 7, Chapter 15) and compensatory uptake and reduction by plants.

Oxidation of reduced species is initiated in the troposphere for the most part by reaction with OH. The critical importance of OH in tropospheric chemistry was first recognized in 1971 by Hiram Levy, then a post-doctoral research fellow at Harvard University. Photolysis of O_3 (reaction 14.15) provides a source of $O(^1D)$; subsequent reaction of $O(^1D)$ with H_2O (reaction 14.23) results in the production of OH. As noted above, oxidation of reduced gases in the troposphere can be associated with either production or consumption of O_3. Whether O_3 is produced or consumed in the course of oxidation depends on the supply of NO. In the absence of NO, oxidation is limited by the supply of O_3; in the presence of NO, oxidation may be associated with significant tropospheric production of O_3.

Conversion of CO to CO_2 may be summarized, as we shall see, by either of the bulk or net reactions:[2]

$$CO + 2O_2 \rightarrow CO_2 + O_3 \qquad (17.1)$$

or

$$CO + O_3 \rightarrow CO_2 + O_2 \qquad (17.2)$$

Similar bifurcation is associated with oxidation of CH_4 and other hydrocarbons. We will be concerned primarily with elaboration of chemical paths for oxidation of reduced gases in the troposphere and with the processes regulating the abundance of O_3. Our focus will be on the mechanisms through which the chemical system in the atmosphere is able to dispose of the rich suite of compounds emitted by industry and by the biosphere, with the self-cleansing feature of the atmosphere noted above. A comprehensive treatment of oxidation presupposes an understanding of sources and sinks for O_3.

In sufficiently high concentration, O_3 can pose a serious problem for human health. It is unclear at what, if any, level O_3 may be considered environmentally benign. Models suggest that in the absence of human activity—specifically, in the absence of industrial sources of NO, CO, and hydrocarbons—ambient levels of O_3 in the troposphere should lie in the range 10–20 ppb. Chronic exposure to O_3 at levels above 50 ppb is known to cause damage to sensitive plants. Levels above 300 ppb are judged serious enough in cities such as Los Angeles to force the issuance of health alerts. Standards for permissible levels of O_3 differ from country to country. The limit is set at 84 ppb in the United States; by comparison, the standard for Switzerland is 60 ppb. Setting standards for O_3 involves necessarily a measure of pragmatism. There is little sense in legislating requirements so strict that they cannot be met; on the other hand, they should be stringent enough to stimulate creative measures to ensure protection of the environment at a reasonable cost.

As we will see, O_3 is formed in urban areas as a product of chemical reactions triggered by local industrial emissions of hydrocarbons and NO_x. Elevated levels of O_3 are also observed in regions that would normally be classified as rural: on occasions, for example, during summer in large areas of the United States east of the Mississippi. Production of O_3 is believed to result in this case from reactions fueled by a combination of natural and anthropogenic inputs; hydrocarbons from trees and NO_x from electric power plants, trucks, and automobiles. As the Governor of California, Ronald Reagan was embroiled in a controversy over the cutting of redwoods and is reputed to have commented that trees cause pollution. He was partially right—and partially wrong. Trees, emitting hydrocarbons, contribute to elevated O_3, but they require a helping hand from sunlight and human agents, specifically a stimulus from industrial sources of NO_x. Setting sensible standards for O_3 and developing realistic strategies for compliance requires a comprehensive appreciation of the complex chemical and physical factors determining the level of O_3 in the lower atmosphere; this chapter is intended to provide a perspective on these issues.

In a sense the atmosphere operates as the immune system of the biosphere. To what extent is this immune system under stress? Is the stress merely local, as indicated by unacceptably high levels of O_3 in cities as diverse as Los Angeles, Mexico City, and São Paulo, or has it expanded to a regional scale as suggested by the data for O_3 in the summertime eastern United States? Abundances of CH_4 have been rising recently at a rate of close to 1% per year. The gas is removed mainly by reaction with OH and has a lifetime in

the atmosphere of about 8.5 yrs. Does the rise in CH_4 reflect, in part at least, a decrease in the globally averaged abundance of OH? Is the growth in CH_4 attributable to a decrease in the potential of the atmosphere to globally dispose of biospheric waste, to a decline in the oxidative or self-cleansing potential of the global immune system? These are the questions that motivate the following discussion.

We begin, in Section 17.1, with an introduction to the processes regulating the abundance of OH. The simple case of oxidation of CO is discussed in Section 17.2. The more complex example of CH_4 is treated in Section 17.3. The chemistry of polluted environments is discussed in Section 17.4. The global distribution of OH and the oxidative potential of the atmosphere are treated in Section 17.5. Global and hemispheric budgets of O_3 and CH_4 are discussed in Sections 17.6 and 17.7 with summary remarks in Section 17.8. We postpone a treatment of the oxidation of sulfur compounds in the context of a discussion of the phenomenon of acid rain until Chapter 18.

17.1 The Chemistry of Tropospheric OH

Photolysis of O_3 yielding $O(^1D)$,

$$h\nu + O_3 \rightarrow O(^1D) + O_2 , \qquad (17.3)$$

provides the essential first step in the production of OH. The rate constant for a photolytic process such as (17.3) depends on the sum (or integral) over wavelength of the product of the cross section for the reaction and the radiative flux: more specifically, on the product of the cross section and the radiance, the intensity of light integrated over all directions (see Section 13.2, as well as Endnote 3 of this chapter). Absorption by O_3 provides the dominant path for attenuation of solar radiation shortward of about 310 nm. As illustrated in Figure 17.1, the cross section for (17.3) is largest near 250 nm. Radiation shortward of 300 nm is strongly absorbed by O_3 in the stratosphere, and relatively little radiation in this spectral range penetrates to the troposphere, as indicated in Figure 17.2a–b. Production of $O(^1D)$ is energetically possible at wavelengths less than about 320 nm. The cross section for (17.3) is negligible, however, longward of 310 nm. It follows that production of $O(^1D)$ in the troposphere is regulated primarily by radiation transmitted in a narrow band of wavelengths between 300–310 nm, as illustrated in Figure 17.3.

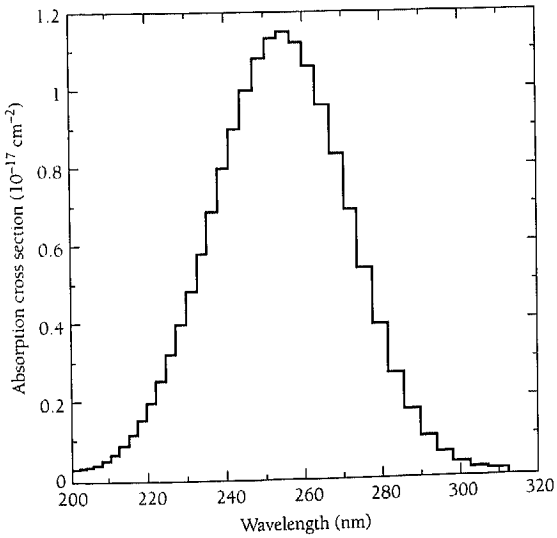

Figure 17.1 Absorption cross section of ozone from 200 to 320 nm.

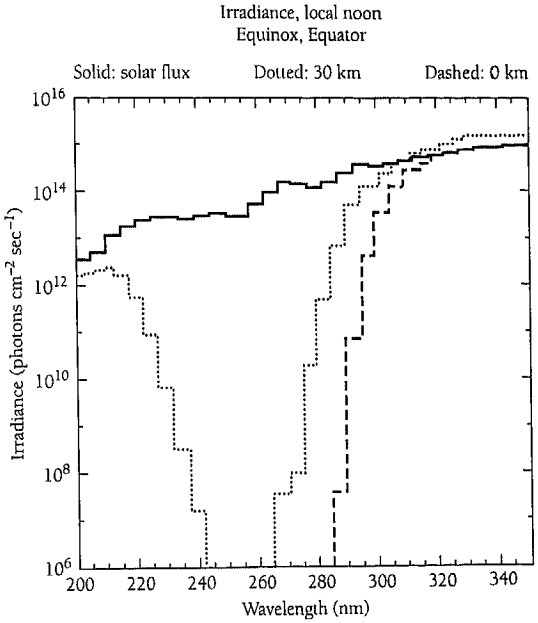

Figure 17.2a Solar irradiance at the equator at equinox, as viewed from outside of the atmosphere (solid line), from 30 km (dotted line), and from the surface (dashed line).

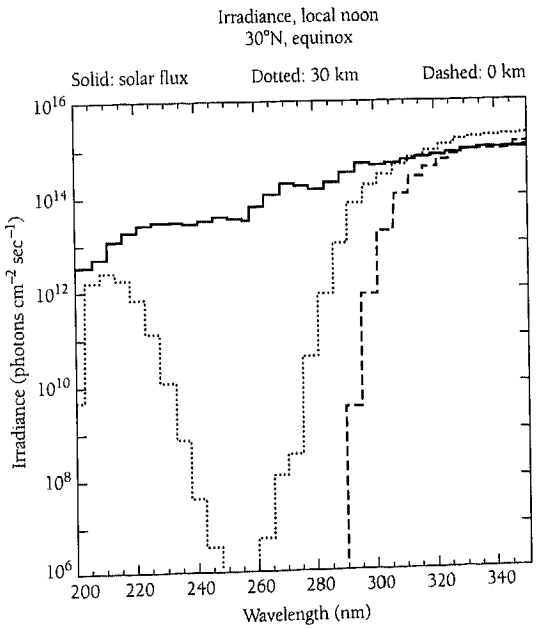

Figure 17.2b Solar irradiance at 30°N at equinox, as viewed from outside the atmosphere (solid line), from 30 km (dotted line), and from the surface (dashed line).

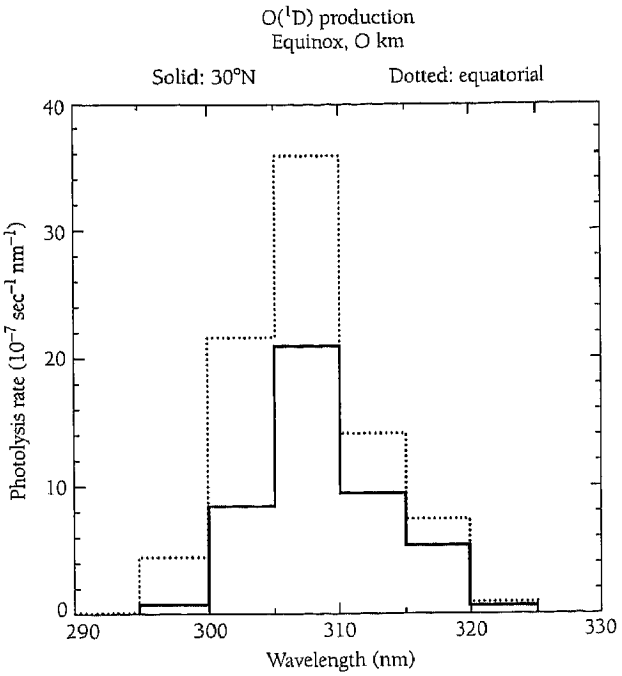

Figure 17.3 Wavelength dependence of ozone photolysis, J_3, for noon under equinoctial conditions near the surface at 30°N (solid line) and at the equator (dotted line).

Example 17.1: Evaluate the contribution of direct solar radiation in the wavelength range 300–310 nm to the rate constant for reaction (17.3) at the equator for conditions corresponding to noon at equinox (solar zenith angle ($\theta = 0$). Assume that the solar flux at the top of the atmosphere in the wavelength bands 300–305 nm and 305–310 nm is given by 3.94×10^{14} and 4.82×10^{14} photons cm^{-2} sec^{-1}, respectively. Radiation is attenuated as a result of absorption by O_3 and Rayleigh scattering by air. The cross sections for absorption by O_3 in the selected wavelength intervals, 300–305 nm and 305–310 nm, are given by 2.47×10^{-19} cm^2 and 1.22×10^{-19} cm^2, respectively. The corresponding cross sections for Rayleigh scattering are 5.47×10^{-26} cm^2 and 5.10×10^{-26} cm^2, respectively. Assume a vertical column density for O_3 of 7.89×10^{18} cm^{-2}, corresponding to an abundance of 294 DU. The column density for air may be taken as 2.15×10^{25} molecules cm^{-2}. Assume that the quantum yield for O(^{1}D), the fraction of photons absorbed by O_3 contributing to production of O(^{1}D), is 1.0 for the interval 300–305 nm and 0.9 for 305–310 nm.

Answer: The first step in this calculation involves evaluation of the optical depth of the atmosphere for the relevant wavelength intervals (see Section 13.1 for a definition of optical depth). For convenience we shall indicate quantities for the 300–305 nm and 305–310 nm intervals by subscripts 1 and 2, respectively:

$$\tau_1 = N_{O_3} Q_{1,O_3} + N_{air} Q_{1,air}$$

$$\tau_2 = N_{O_3} Q_{2,O_3} + N_{air} Q_{2,air},$$

where Q_{i,O_3} denotes the cross sections for absorption of radiation in wavelength interval i by O_3, $Q_{i,air}$ is the corresponding cross section for scattering by air, and N_{O_3} and N_{air} are the vertical column densities for O_3 and air molecules, respectively.

Substituting the appropriate values for cross sections and column densities, we find

$$\tau_1 = [(7.89 \times 10^{18}\ \text{cm}^{-2})(2.47 \times 10^{-19}\ \text{cm}^2)] + [(2.15 \times 10^{25}\ \text{cm}^{-2})(5.47 \times 10^{-26}\ \text{cm}^2)]$$

$$= 3.12$$

$$\tau_2 = [(7.89 \times 10^{18}\ \text{cm}^{-2})(1.22 \times 10^{-19}\ \text{cm}^2)] + [(2.15 \times 10^{25}\ \text{cm}^{-2})(5.10 \times 10^{-26}\ \text{cm}^2)]$$

$$= 2.06$$

The flux of solar radiation at the surface in the wavelength intervals 1 and 2 is given by

$$F_1 = F_1^\infty \exp(-\tau_1)$$

$$= (3.94 \times 10^{14}\ \text{photons cm}^{-2}\ \text{sec}^{-1})(4.37 \times 10^{-2})$$

$$= 1.72 \times 10^{13}\ \text{photons cm}^{-2}\ \text{sec}^{-1}$$

and

$$F_2 = F_2^\infty \exp(-\tau_2)$$

$$= (4.82 \times 10^{14}\ \text{photons cm}^{-2}\ \text{sec}^{-1})(1.27 \times 10^{-1})$$

$$= 6.14 \times 10^{13}\ \text{photons cm}^{-2}\ \text{sec}^{-1},$$

where F_i^∞ defines the appropriate value for the flux at the top of the atmosphere. The contribution, J_3^i, to the rate constant for (17.3) from wavelength interval i is given by

$$J_3^i = E_i^\infty Q_{i,O_3} F_i,$$

where E_i is the quantum yield. Substituting appropriate values for E_i, Q_{i,O_3}, and F_i, we find:

$$J_3^1 = (1.0)(2.47 \times 10^{-19}\ \text{cm}^2)(1.72 \times 10^{13}\ \text{photons cm}^{-2}\ \text{sec}^{-1})$$

$$= 4.25 \times 10^{-6}\ \text{sec}^{-1}$$

$$J_3^2 = (0.9)(1.22 \times 10^{-19}\ \text{cm}^2)(6.14 \times 10^{13}\ \text{photons cm}^{-2}\ \text{sec}^{-1})$$

$$= 6.74 \times 10^{-6}\ \text{sec}^{-1}$$

The aggregate value for J_3 is obtained by summing over the contributing wavelength intervals:

$$J_3 = (4.25 \times 10^{-6} + 6.74 \times 10^{-6})\ \text{sec}^{-1}$$

$$= 1.10 \times 10^{-5}\ \text{sec}^{-1}$$ ■

Example 17.2: Repeat the calculation described in Example 17.1, ignoring effects of Rayleigh scattering in limiting penetration of solar radiation. The calculation in Example 17.1 implicitly assumes that scattered photons are no longer available to carry out reaction (17.3), meaning, scattering is treated as though it were an absorptive process. The results in Example

(17.1) should thus represent a lower limit for the contribution of radiation in the wavelength interval 300–310 nm to the rate constant for (17.3). The present calculation would be appropriate if scattering were to take place mainly in the forward direction. In practice, the Rayleigh mechanism predicts that scattering should proceed with comparable probability in the forward and backward directions.

Answer: The values of τ_1 and τ_2 are given in this case by the first terms in the expressions derived for these quantities in Example 17.1:

$$\tau_1 = 1.95$$

$$\tau_2 = 0.96$$

It follows that

$$F_1 = (3.94 \times 10^{14} \text{ photons cm}^{-2} \text{ sec}^{-1})(1.42 \times 10^{-1})$$
$$= 5.59 \times 10^{13} \text{ photons cm}^{-2} \text{ sec}^{-1}$$

$$F_2 = (4.82 \times 10^{14} \text{ photons cm}^{-2} \text{ sec}^{-1})(3.83 \times 10^{-1})$$
$$= 1.85 \times 10^{14} \text{ photons cm}^{-2} \text{ sec}^{-1}$$

$$J_3^1 = (1.0)(2.47 \times 10^{-19} \text{ cm}^2) \times (5.59 \times 10^{13} \text{ photons cm}^{-2} \text{ sec}^{-1}) = 1.39 \times 10^{-5}$$

$$J_3^2 = (0.9)(1.22 \times 10^{-19} \text{ cm}^2) \times (1.85 \times 10^{14} \text{ photons cm}^{-2} \text{ sec}^{-1}) = 2.03 \times 10^{-5}$$

$$J_3 = (1.39 \times 10^{-5} + 2.03 \times 10^{-5}) \text{ sec}^{-1}$$
$$= 3.42 \times 10^{-5} \text{ sec}^{-1}$$ ■

The probability that scattering should take place into a direction inclined at an angle θ with respect to the direction of incidence of the light is defined by a quantity known as the **phase function**. The phase function for Rayleigh scattering is given by 3/4 (1+ $\cos^2 \theta$). Forward scattering corresponds to $\theta = 0$, while backward scattering is defined by $\theta = 180°$. According to the Rayleigh phase function, scattering at 90° to the direction of incidence is only half as probable as scattering in either the forward or backward direction. Effects of scattering on photolysis are schematically illustrated in Figure 17.4. Figure 17.4 depicts a situation for which molecules in a representative volume of air near the surface are exposed to a combination of directly transmitted solar radiation, radiation reflected from the surface, radiation scattered once by air molecules (case a), and radiation that is scattered twice (case b).

In practice, the approach adopted in Example 17.2, where effects of scattering are completely ignored, results in a slight overestimate in the values derived for J_3. Also, in the examples above, we omitted contributions to photolysis from shorter and longer wavelengths. This procedure results in an underestimate, by about 30%, in the value derived for J_3. A more detailed calculation, accounting for scattering and allowing for a reasonable reflectivity for the surface (appropriate for an albedo of 0.1), indicates a value for J_3 corresponding to the overhead Sun at the equator of about 4.2×10^{-5} sec^{-1} for the conditions envisaged in Examples 17.1 and 17.2.

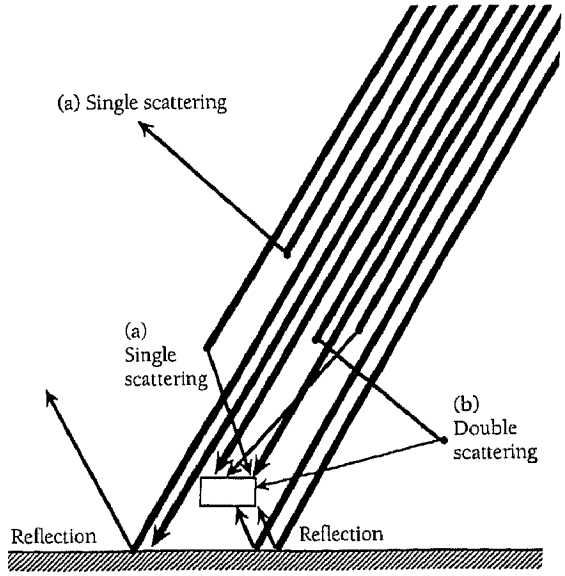

Figure 17.4 Pathways of incoming sunlight.

The key reactions regulating the abundance of tropospheric $O(^1D)$ and production of OH, in addition to (17.3), are

$$O(^1D) + N_2 \rightarrow O(^3P) + N_2, \quad (17.4)$$

$$O(^1D) + O_2 \rightarrow O(^3P) + O_2, \quad (17.5)$$

and

$$O(^1D) + H_2O \rightarrow OH + OH \quad (17.6)$$

Adopting the notation used in Chapters 13 through 15, with rate constants for (17.4)–(17.6) denoted by k_4–k_6, the abundance of $O(^1D)$ may be obtained by balancing the rate for production by (17.3) with the rate for removal by (17.4)–(17.6). Thus,

$$J_3[O_3] = [O(^1D)]\ (k_4[N_2] + k_5[O_2] + k_6\ [H_2O]) \quad (17.7)$$

It follows that

$$[O(^1D)] = \frac{J_3[O_3]}{k_4[N_2] + k_5[O_2] + k_6[H_2O]} \quad (17.8)$$

The third term in the denominator of (17.8) typically accounts for 10% or less of the combined contribution to quenching from N_2 and O_2. The relative abundances of N_2 and O_2 are constant, and it is convenient to define an effective rate constant for quenching of $O(^1D)$ by air, according to the relation:

$$k^*[M] = k_4[N_2] + k_5[O_2] \quad (17.9)$$

In this case, (17.8) may be written in the simpler form:

$$[O(^1D)] = \frac{J_3[O_3]}{k^*[M]} \quad (17.10)$$

With typical values for k_4–k_6 (see Table 17.1), the rate for production of OH, $p(OH)$, is given by

Table 17.1 Rate Constants for the Key Reactions Involved in HO_x Chemistry

Reaction	Equatorial		Midlatitudes	
	0 km (T = 300 K)	*5 km (T = 272 K)*	*0 km (T = 292 K)*	*5 km (T = 266 K)*
$O_3 + h\nu \rightarrow O(^1D) + O_2$	4.33×10^{-5} sec^{-1}	6.63×10^{-5} sec^{-1}	2.36×10^{-5} sec^{-1}	3.77×10^{-5} sec^{-1}
$O(^1D) + N_2 \rightarrow O + N_2$	2.60×10^{-11} cm^3 sec^{-1}	2.70×10^{-11} cm^3 sec^{-1}	2.62×10^{-11} cm^3 sec^{-1}	2.72×10^{-11} cm^3 sec^{-1}
$O(^1D) + O_2 \rightarrow O + O_2$	4.04×10^{-11} cm^3 sec^{-1}	4.14×10^{-11} cm^3 sec^{-1}	4.06×10^{-11} cm^3 sec^{-1}	4.16×10^{-11} cm^3 sec^{-1}
$O(^1D) + M \rightarrow O + M$	2.87×10^{-11} cm^3 sec^{-1}	2.97×10^{-11} cm^3 sec^{-1}	2.90×10^{-11} cm^3 sec^{-1}	3.00×10^{-11} cm^3 sec^{-1}
$O(^1D) + H_2O \rightarrow OH + OH$	2.20×10^{-10} cm^3 sec^{-1}	2.20×10^{-10} cm^3 sec^{-1}	2.20×10^{-10} cm^3 sec^{-1}	2.20×10^{-10} cm^3 sec^{-1}
$OH + CO \rightarrow H + CO_2$	2.40×10^{-13} cm^3 sec^{-1}	1.99×10^{-13} cm^3 sec^{-1}	2.40×10^{-13} cm^3 sec^{-1}	1.99×10^{-13} cm^3 sec^{-1}
$OH + CH_4 \rightarrow CH_3 + H_2O$	6.74×10^{-15} cm^3 sec^{-1}	3.62×10^{-15} cm^3 sec^{-1}	5.71×10^{-15} cm^3 sec^{-1}	3.11×10^{-15} cm^3 sec^{-1}
$OH + O_3 \rightarrow HO_2 + O_2$	6.98×10^{-14} cm^3 sec^{-1}	5.07×10^{-14} cm^3 sec^{-1}	6.41×10^{-14} cm^3 sec^{-1}	4.68×10^{-14} cm^3 sec^{-1}
$OH + NO_2 + M \rightarrow HNO_3 + M$	4.63×10^{-31} cm^6 sec^{-1}	7.57×10^{-31} cm^6 sec^{-1}	4.79×10^{-31} cm^6 sec^{-1}	7.87×10^{-31} cm^6 sec^{-1}
$HO_2 + O_3 \rightarrow OH + NO_2$	2.08×10^{-15} cm^3 sec^{-1}	1.75×10^{-15} cm^3 sec^{-1}	1.99×10^{-15} cm^3 sec^{-1}	1.68×10^{-15} cm^3 sec^{-1}
$HO_2 + NO \rightarrow OH + NO_2$	8.51×10^{-12} cm^3 sec^{-1}	9.27×10^{-12} cm^3 sec^{-1}	8.71×10^{12} cm^3 sec^{-1}	9.46×10^{-12} cm^3 sec^{-1}
$NO + O_3 \rightarrow NO_2 + O_2$	1.89×10^{-14} cm^3 sec^{-1}	1.17×10^{-14} cm^3 sec^{-1}	1.66×10^{-14} cm^3 sec^{-1}	1.04×10^{-14} cm^3 sec^{-1}
$NO_2 + h\nu \rightarrow NO + O$	8.67×10^{-3} sec^{-1}	1.14×10^{-2} sec^{-1}	7.92×10^{-3} sec^{-1}	1.09×10^{-2} sec^{-1}
$HO_2 + OH \rightarrow H_2O + O_2$	1.10×10^{-10} cm^3 sec^{-1}	1.20×10^{-10} cm^3 sec^{-1}	1.13×10^{-10} cm^3 sec^{-1}	1.23×10^{-10} cm^3 sec^{-1}
$HO_2 + HO_2 \rightarrow H_2O_2 + O_2$	1.70×10^{-12} cm^3 sec^{-1}	2.08×10^{-12} cm^3 sec^{-1}	1.79×10^{-12} cm^3 sec^{-1}	2.19×10^{-12} cm^3 sec^{-1}
$HO_2 + HO_2 + M \rightarrow H_2O_2 + O_2 + M$	4.75×10^{-32} cm^3 sec^{-1}	6.70×10^{-32} cm^3 sec^{-1}	5.21×10^{-32} cm^3 sec^{-1}	7.29×10^{-32} cm^3 sec^{-1}
$H_2O_2 + h\nu \rightarrow OH + OH$	8.30×10^{-6} sec^{-1}	1.18×10^{-5} sec^{-1}	6.50×10^{-6} sec^{-1}	9.99×10^{-6} sec^{-1}
$H_2O_2 + OH \rightarrow HO_2 + H_2O$	1.70×10^{-12} cm^3 sec^{-1}	1.61×10^{-12} cm^3 sec^{-1}	1.68×10^{-12} cm^3 sec^{-1}	1.59×10^{-12} cm^3 sec^{-1}

$$p(\mathrm{OH}) = 2k_6[\mathrm{H_2O}][\mathrm{O}(^1\mathrm{D})]$$

$$= \frac{2k_6[\mathrm{H_2O}]J_3[\mathrm{O_3}]}{k^*[\mathrm{M}]}$$

$$= 2\frac{k_6}{k^*}f_{\mathrm{H_2O}}J_3[\mathrm{O_3}] \qquad (17.11)$$

$$\approx 15 f_{\mathrm{H_2O}}J_3[\mathrm{O_3}]$$

Example 17.3: Repeat the calculation outlined in Example 17.2 for noon at 30°N for equinox. Assume a column density for O_3 of 350 DU, corresponding to an abundance of 9.38×10^{18} mol cm^{-2}. Assume, as before, a column density for air of 2.15×10^{25} cm^{-2}.

Answer: The solar zenith angle at noon corresponding to these conditions is 30° ($\cos\theta = \mu = 0.866$; see Example 17.2).

$$\tau_1 = (9.38 \times 10^{18}\ \mathrm{cm^{-2}})\ (2.47 \times 10^{-19}\ \mathrm{cm^2})$$

$$= 2.32$$

$$\tau_2 = (9.38 \times 10^{18}\ \mathrm{cm^{-2}})\ (1.22 \times 10^{-19}\ \mathrm{cm^2})$$

$$= 1.14$$

$$F_1 = F_1^\infty \exp\left(-\frac{\tau_1}{.866}\right)$$

$$= (3.94 \times 10^{14}\ \mathrm{photons\ cm^{-2}\,sec^{-1}})\ \exp\left(\frac{-2.32}{.866}\right)$$

$$= (3.94 \times 10^{14}\ \mathrm{photons\ cm^{-2}\ sec^{-1}})\ (6.86 \times 10^{-2})$$

$$= 2.70 \times 10^{13}\ \mathrm{photons\ cm^{-2}\ sec^{-1}}$$

$$F_2 = (4.82 \times 10^{14}\ \mathrm{photons\ cm^{-2}\ sec^{-1}})\ \exp\left(\frac{-1.14}{.866}\right)$$

$$= (4.82 \times 10^{14}\ \mathrm{photons\ cm^{-2}\ sec^{-1}})\ (2.68 \times 10^{-1})$$

$$= 1.29 \times 10^{14}\ \mathrm{photons\ cm^{-2}\ sec^{-1}}$$

$$J_3^1 = (1.0)(2.47 \times 10^{-19}\ \mathrm{cm^2}) \times (2.70 \times 10^{13}\ \mathrm{photons\ cm^{-2}\ sec^{-1}})$$

$$= 6.67 \times 10^{-6}\ \mathrm{sec^{-1}}$$

$$J_3^2 = (0.9)(1.22 \times 10^{-19}\ \mathrm{cm^2}) \times (1.29 \times 10^{14}\ \mathrm{photons\ cm^{-2}\ sec^{-1}})$$

$$= 1.41 \times 10^{-5}\ \mathrm{sec^{-1}}$$

$$J_3 = 2.08 \times 10^{-5}\ \mathrm{sec^{-1}}$$

A more precise calculation for J_3, allowing for scattering and contributions from other wavelengths, yields a value of 2.36×10^{-5} sec^{-1}. ■

Example 17.4: Estimate the rate for production of OH at the surface at 30°N latitude for noon at equinox. Assume a mixing ratio for H_2O of 1.7×10^{-2} corresponding to a relative humidity of about 80% at a temperature of about 290 K. Assume a mixing ratio for O_3 of 50 ppb, typical for relatively clean rural areas of the United States. Assume a value of 2.4×10^{-5} sec^{-1} for J_3 appropriate for a column density of O_3 of about 350 DU. The total density of air molecules, M, may be taken as 2.5×10^{19} cm^{-3}.

Answer:

$$\begin{aligned} p(\mathrm{OH}) &= 15 f_{H_2O} J_3 [O_3] \\ &= 15 f_{H_2O} J_3 f_{O_3} [M] \\ &= (1.5 \times 10^1)(1.7 \times 10^{-2})(2.4 \times 10^{-5}\ \mathrm{sec}^{-1}) \\ &\quad \times (5 \times 10^{-8})(2.5 \times 10^{19}\ \mathrm{cm}^{-3}) \\ &= 7.7 \times 10^6\ \mathrm{cm}^{-3}\ \mathrm{sec}^{-1} \end{aligned}$$

■

Example 17.5: Estimate the abundance of $O(^1D)$ for the conditions defined in Example 17.4. Assume a value for k^* of 3×10^{-11} cm^3 sec^{-1}.

Answer: The concentration of $O(^1D)$ may be evaluated to an adequate approximation using equation (17.10):

$$\begin{aligned} [O^1D] &= \frac{J_3[O_3]}{k^*[M]} \\ &= \frac{J_3}{k^*} f_{O_3} \\ &= \frac{(2.4 \times 10^{-5}\mathrm{sec}^{-1})(5 \times 10^{-8})}{3 \times 10^{-11}\ \mathrm{cm}^3\ \mathrm{sec}^{-1}} \\ &= 4 \times 10^{-2}\ \mathrm{cm}^{-3} \end{aligned}$$

■

Example 17.6: Calculate the lifetime of $O(^1D)$ at the surface for the conditions defined in Example 17.4.

Answer: The lifetime, $\tau(O(^1D))$, for $O(^1D)$ is determined primarily by the rate at which the species is quenched by air (converted to the ground state form of the atom, $O(^3P)$):

$$\begin{aligned} \tau &= (k^*[M])^{-1} \\ &= \frac{1}{(3 \times 10^{-11}\mathrm{cm}^3\ \mathrm{sec}^{-1})(2.5 \times 10^{19}\ \mathrm{cm}^{-3})} \\ &= 1.3 \times 10^{-9}\ \mathrm{sec} \end{aligned}$$

■

It is a remarkable fact that the source of OH and, as a consequence, the oxidative potential of the troposphere are controlled in the final analysis by the concentration of a metastable atom, a species whose lifetime in the troposphere is typically less than about 10^{-8} sec (the lifetime is longer in the upper troposphere than at the surface, reflecting the inverse dependence of the lifetime on density, as indicated in Example 17.6). The concentration of tropospheric $O(^1D)$ is essentially undetectable: it corresponds to a mixing ratio of less than 10^{-20}.

As indicated by (17.11), production of tropospheric OH depends on the abundance of tropospheric O_3, on the mixing ratio of tropospheric H_2O, and on the value of J_3. The rate constant J_3 is sensitive in turn to the magnitude of the solar zenith angle (time of day) and to the overhead (primarily stratospheric) column abundance of O_3.[4] Values of J_3 are presented in Figure 17.5 for a range of column densities of O_3 at the equator and at 30°N for solar zenith angles appropriate for noon at equinox.[5]

As illustrated in Figure 17.6, the chemistry of OH is inextricably linked to a suite of reactions involving H, HO_2, and H_2O_2 identified as the key components of the tropospheric HO_x family. Reaction with CO provides an important sink for tropospheric OH, with additional contributions from reactions involving CH_4 and H_2O_2:

$$\mathrm{OH} + \mathrm{CO} \rightarrow \mathrm{H} + \mathrm{CO_2}, \qquad (17.12)$$

$$\mathrm{OH} + \mathrm{CH_4} \rightarrow \mathrm{H_2O} + \mathrm{CH_3}, \qquad (17.13)$$

and

$$\mathrm{OH} + \mathrm{H_2O_2} \rightarrow \mathrm{H_2O} + \mathrm{HO_2} \qquad (17.14)$$

The H atom produced in (17.12) is immediately converted to HO_2 by

$$\mathrm{H} + \mathrm{O_2} + \mathrm{M} \rightarrow \mathrm{HO_2} + \mathrm{M} \qquad (17.15)$$

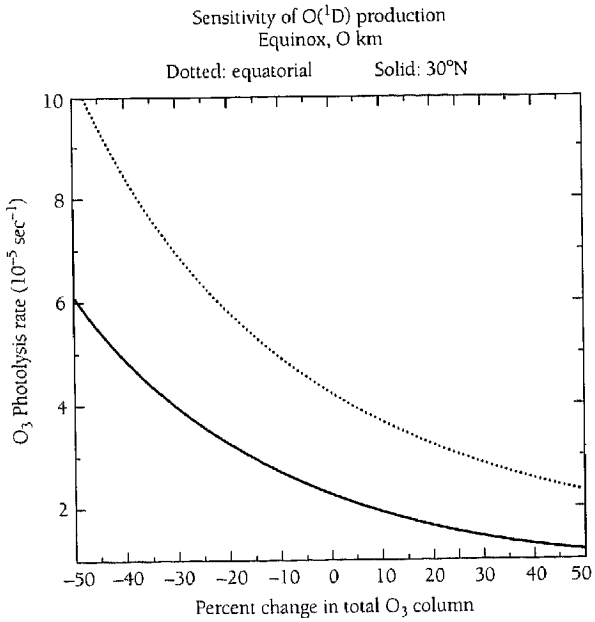

Figure 17.5 Sensitivity of ozone photolysis (J_3) near the surface, at the equator (dotted line), and at 30°N (solid line) to the total column density of ozone. Values are calculated for equinoctial conditions at noon with an equatorial ozone column of 294 DU and a midlatitude ozone column of 343 DU.

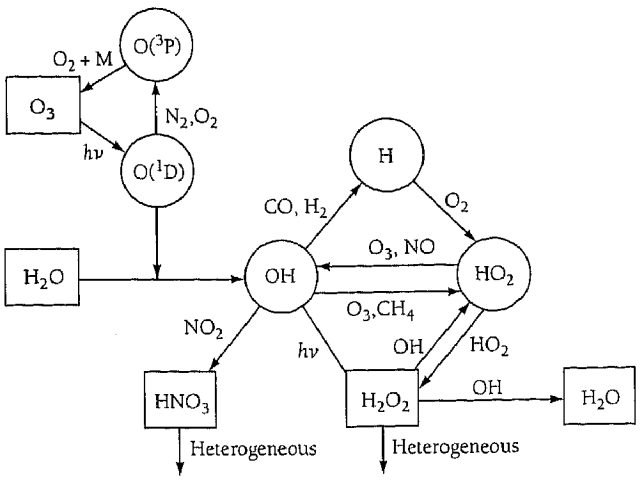

Figure 17.6 Chemical pathways responsible for the production, loss, and partitioning of HO_x.

HO_2 may be cycled back to OH by reactions with NO or O_3,

$$HO_2 + NO \rightarrow OH + NO_2 \qquad (17.16)$$

and

$$HO_2 + O_3 \rightarrow OH + 2O_2, \qquad (17.17)$$

or it may be transformed to H_2O_2 by

$$HO_2 + HO_2 \rightarrow H_2O_2 + O_2 \qquad (17.18)$$

H_2O_2 is removed by photolysis

$$h\nu + H_2O_2 \rightarrow 2OH \qquad (17.19)$$

by reaction with OH, (17.14), and by heterogeneous reactions, either at the surface or on particles (mainly droplets of water) in the atmosphere:

$$H_2O_2 \rightarrow \text{products} \qquad (17.20)$$

Reactions (17.14) and (17.20) provide sinks for two molecules of odd hydrogen (for this purpose H_2O_2 is assumed to represent a pair of HO_x species). Reaction of OH with NO_2 forming HNO_3,

$$OH + NO_2 + M \rightarrow HNO_3 + M, \qquad (17.21)$$

followed by heterogeneous removal of HNO_3 contributes an additional sink for HO_x. One molecule of HO_x is removed in (17.13): on the other hand, (17.13) represents but the first step in oxidation of CH_4. It provides no net sink for radicals; the radical OH is merely replaced by the methyl radical CH_3. Oxidation of CH_4, as we shall see, can represent either a source or a sink for two molecules of HO_x or it may be neutral. The impact of CH_4 oxidation on the abundance of HO_x critically depends on the supply of NO_x.

Example 17.7: Estimate the relative importance of (17.12) and (17.13) as sinks for OH at the surface at 30°N latitude. Assume mixing ratios for CO and CH_4 of 10^{-7} and 1.7×10^{-6}, respectively, with a total air density of 2.5×10^{19} mol cm^{-3}.

Answer: The rates (cm^{-3} sec^{-1}) at which OH is removed by (17.12) and (17.13) are given by

$$R_{12} = k_{12}\,[OH][CO]$$

and

$$R_{13} = k_{13}\,[OH][CH_4]$$

Where k_{12} and k_{13} are the rate constants for (17.12) and (17.13), respectively. The relative importance of (17.12) and (17.13) depends on the values of the corresponding loss frequencies:

$$\nu_{12} = k_{12}[CO] = k_{12} f_{CO}[M]$$

and

$$\nu_{13} = k_{13}[CH_4] = k_{13}\, f_{CH_4}\,[M]$$

The ratio ν_{12} to ν_{13} is given by

$$\frac{\nu_{12}}{\nu_{13}} = \frac{k_{12} f_{CO}}{k_{13} f_{CH_4}}$$

Using values presented in *Table 17.1* to substitute for k_{12} and k_{13}, with values for f_{CO} and f_{CH_4} as specified:

$$\frac{\nu_{12}}{\nu_{13}} = \frac{\left(2.4\times10^{-13}\ \text{cm}^3\ \text{sec}^{-1}\right)\left(10^{-7}\right)}{\left(5.7\times10^{-15}\ \text{cm}^3\ \text{sec}^{-1}\right)\left(1.7\times10^{-6}\right)}$$

$$= 2.5$$

It follows that (17.12) is 2.5 times more important than (17.13) as a sink for OH. ■

Example 17.8: Estimate the relative importance of (17.16) and (17.17) as sinks for HO_2 at the surface at 30°N equinox. Assume mixing ratios for NO and O_3 of 5×10^{-12} and 5×10^{-8}, respectively, values typical for noon under relatively clean (low NO_x, low O_3) rural conditions.

Answer: Writing rate constants for (17.16) and (17.17) as k_{16} and k_{17}, respectively,

$$\nu_{16} = k_{16}\,[NO] = k_{16} f_{NO}\,[M]$$

$$\nu_{17} = k_{17}\,[O_3] = k_{17} f_{O3}\,[M]$$

$$\frac{\nu_{17}}{\nu_{16}} = \frac{k_{17} f_{O_3}}{k_{16} f_{NO}}$$

$$= \frac{(2.0 \times 10^{-15}\ \text{cm}^3\ \text{sec}^{-1})(5 \times 10^{-8})}{(8.7 \times 10^{-12}\ \text{cm}^3\ \text{sec}^{-1})(5 \times 10^{-12})}$$

$$= 2.3$$

With our assumptions, removal of HO_2 by O_3 is 2.3 times more efficient than removal by NO. ■

Example 17.9: For conditions defined in Example 17.8, estimate the density of HO_2 for which the rate for removal of HO_2 by (17.18) is comparable to the rate for removal by (17.17).

Answer:

$$R_{17} = k_{17}\,[HO_2][O_3]$$

$$R_{18} = k_{18}\,[HO_2]^2$$

Equal values for R_{17} and R_{18} imply

$$k_{17}\,[HO_2][O_3] = k_{18}\,[HO_2]^2$$

It follows that

$$[HO_2] = k_{17}\,[O_3]\,/\,k_{18}$$

$$= \frac{(2.0 \times 10^{-15}\ \text{cm}^3\ \text{sec}^{-1})(5 \times 10^{-8} \times 2.5 \times 10^{19}\ \text{cm}^{-3})}{(1.8 \times 10^{-12}\ \text{cm}^3\ \text{sec}^{-1} + 1.3 \times 10^{-12}\ \text{cm}^3\ \text{sec}^{-1})}$$

$$= \frac{(2.0 \times 10^{-15}\ \text{cm}^3\ \text{sec}^{-1})(1.25 \times 10^{11}\ \text{cm}^{-3})}{(3.1 \times 10^{-12}\ \text{cm}^3\ \text{sec}^{-1})}$$

$$= 8.1 \times 10^7\ \text{cm}^{-3}$$ ■

The value of k_{18} used here and in subsequent examples accounts for the influence of the three-body reaction, $HO_2 + HO_2 + M \rightarrow H_2O_2 + O_2 + M$, included in Table 17.1. If the concentration of HO_2 is larger than 10^8 cm^{-3}, production of H_2O_2 is more important than cycling back to OH as a sink for HO_2.

Example 17.10: To estimate the abundance of HO_2, assume that HO_x is removed mainly by (17.14) and (17.20). Assume further that photolysis of H_2O_2, reaction (17.19), is less important than (17.14) and (17.20) as a sink for H_2O_2. Under these circumstances, the rate for production of HO_x by (17.6) should equal the rate at which HO_2 is converted to H_2O_2. Estimate the abundance of HO_2 at 30°N equinox, noon, using the HO_x production rate calculated in Example 17.4.

Answer: According to Example 17.4, the rate for production of HO_x is given by

$$p(HO_x) = 7.7 \times 10^6\ \text{cm}^{-3}\ \text{sec}^{-1}$$

and

$$L(HO_x) = 2k_{18}\,[HO_2]^2,$$

where the factor of two accounts for the fact that two molecules of HO_x are removed by (17.18), followed by (17.14) or (17.20). Equating rates for production and loss,

$$7.7 \times 10^6\ \text{cm}^{-3}\ \text{sec}^{-1} = 2k_{18}\,[HO_2]^2$$

$$= 2(3.1 \times 10^{-12}\ \text{cm}^3\ \text{sec}^{-1})[HO_2]^2,$$

it follows that

$$[HO_2]^2 = \frac{7.7 \times 10^6\ \text{cm}^{-3}\ \text{sec}^{-1}}{6.2 \times 10^{-12}\ \text{cm}^{-3}\ \text{sec}^{-1}}$$

$$= 1.24 \times 10^{18}\ \text{cm}^{-6}$$

Thus

$$[HO_2] = 1.1 \times 10^9\ \text{cm}^{-3}$$ ■

The efficiency of reactions such as (17.16), (17.17), and (17.19) in cycling HO_2 and H_2O_2 back to OH may be conveniently measured in terms of a quantity known as the *chain length* for the HO_x cycle. We define the chain length, C, for the HO_x cycle as the ratio of the total rate for production of OH (including contributions from recycling) to the rate for production, solely reflecting the contribution from the primary source (17.6). Allowing for recycling of OH by (17.16), (17.17), and (17.19),

$$C = \big(2k_6[O(^1D)][H_2O] + k_{16}[NO][HO_2] + k_{17}[O_3][HO_2] + 2J_{19}[H_2O_2]\big) / 2k_6[O(^1D)][H_2O], \qquad (17.22)$$

where J_{19} defines the rate constant (sec^{-1}) for (17.19). A chain length greater than 1.0 implies that recycling is important. A chain length close to 1.0 implies that recycling is unimportant. The concentration of OH is given to an adequate approximation in this case by equating the rate for production of OH by (17.6) with the rate for removal, mainly by (17.12) and (17.13):

$$2k_6[O(^1D)][H_2O] = k_{12}\,[OH][CO] + k_{13}\,[OH][CH_4] \qquad (17.23)$$

It follows that

$$[OH] = \frac{2k_6[O(^1D)][H_2O]}{k_{12}[CO] + k_{13}[CH_4]} \qquad (17.24)$$

Allowing for recycling,

$$[OH] = C\left(\frac{2k_6[O(^1D)][H_2O]}{k_{12}[CO] + k_{13}[CH_4]}\right) \qquad (17.25)$$

Using (17.10) to substitute for $[O^1D]$, we may rewrite (17.25) in the form

$$[OH] = C\left\{\frac{2k_6 J_3 f_{O_3} f_{H_2O}}{k^*(k_{12} f_{CO} + k_{13} f_{CH_4})}\right\} \qquad (17.26)$$

The discussion in Examples (17.8)–(17.10), considering cycling of HO_2 back to OH, suggests a chain length close to 1.0 for conditions as defined there for the surface at equinox at 30°N.

Example 17.11: Estimate the concentration of OH for the surface at 30°N for noon at equinox. Assume the value derived in Example 17.4 for production of OH by (17.6), a chain length of 1.0, and mixing ratios for CO and CH_4 of 10^{-7} and 1.7×10^{-6}, as adopted in Example (17.7).

Answer: The concentration of OH is given by

$$[\mathrm{OH}] = \frac{2k_6[\mathrm{O}(^1\mathrm{D})][\mathrm{H_2O}]}{k_{12}[\mathrm{CO}] + k_{13}[\mathrm{CH_4}]}$$

$$= \frac{p(\mathrm{OH})}{\nu_{12} + \nu_{13}}$$

$$= \frac{p(\mathrm{OH})}{[k_{12}f_{\mathrm{CO}} + k_{13}f_{\mathrm{CH_4}}][\mathrm{M}]}$$

$$= \frac{7.7 \times 10^6 \text{ cm}^{-3} \text{ sec}^{-1}}{(2.4 \times 10^{-20} \text{ cm}^3 \text{ sec}^{-1} + 9.7 \times 10^{-21} \text{ cm}^3 \text{ sec}^{-1})(2.5 \times 10^{19} \text{ cm}^{-3})}$$

$$= \frac{7.7 \times 10^6}{(3.4 \times 10^{-20})(2.5 \times 10^{19})}$$

$$= 9 \times 10^6 \text{cm}^{-3}$$ ■

Example 17.12: For conditions defined in Example 17.11, estimate the lifetime of OH.

Answer: The lifetime $\tau(\mathrm{OH})$ is given by

$$\tau(\mathrm{OH}) = \frac{[\mathrm{OH}]}{p(\mathrm{OH})}$$

$$= \frac{9 \times 10^6 \text{ cm}^{-3}}{7.7 \times 10^6 \text{ cm}^{-3}\text{sec}^{-1}}$$

$$= 1.2 \text{ sec}$$ ■

Example 17.13: With the assumptions stated in Example 17.10, estimate the lifetime for HO_2.

Answer: The lifetime $\tau(\mathrm{HO_2})$ is given by

$$\tau(\mathrm{HO_2}) = \frac{[\mathrm{HO_2}]}{p(\mathrm{HO_2})}$$

But with our assumptions, $p(\mathrm{OH}) = p(\mathrm{HO_2})$.

Thus,

$$\tau(\mathrm{HO_2}) = \frac{1.1 \times 10^9 \text{ cm}^{-3}}{7.7 \times 10^6 \text{ cm}^{-3} \text{ sec}^{-1}}$$

$$= 1.4 \times 10^2 \text{ sec}$$

The lifetime for HO_2 is about two minutes. ■

Example 17.14: Estimate the relative importance of (17.14), (17.19), and (17.20) as sinks for H_2O_2. For this purpose, use the density of OH calculated in Example 17.12 and assume a loss frequency of 2.3×10^{-6} sec^{-1} for the heterogeneous process (17.20).

Answer: The relative importance of (17.14), (17.19), and (17.20) are given by the corresponding loss frequencies:

$$\nu_{14} = k_{14}\,[\mathrm{OH}],$$

$$\nu_{19} = J_{19},$$

and

$$\nu_{20} = 2.3 \times 10^{-6} \text{ sec}^{-1},$$

where k_{14} is the rate constant for (17.14).

Using the values for the rate constants given in Table 17.1,

$$\nu_{19} = 6.5 \times 10^{-6} \text{ sec}^{-1}$$

and

$$\nu_{14} = (1.7 \times 10^{-12} \text{ cm}^3 \text{ sec}^{-1})(9 \times 10^6 \text{ cm}^{-3})$$

$$= 1.5 \times 10^{-5} \text{ sec}^{-1}$$ ■

It follows that reaction (17.14) is the dominant path for removal of H_2O_2. It is about seven times more efficient than the heterogeneous process (17.20) and twice as important as photolysis, reaction (17.19).

Example 17.15: Calculate the density and lifetime of H_2O_2, assuming that H_2O_2 is removed by (17.14), (17.19), and (17.20), with rates implied by the data in Example (17.14). Estimate the rate for production of H_2O_2, using the concentration of HO_2 obtained in Example 17.10.

Answer: The rate for production of H_2O_2 is given by

$$p(\mathrm{H_2O_2}) = k_{18}[\mathrm{HO_2}]^2$$

$$= 3.8 \times 10^6 \text{ cm}^{-3} \text{ sec}^{-1}$$

The loss rate is given by

$$\mathrm{L}(\mathrm{H_2O_2}) = [\mathrm{H_2O_2}]\ (\nu_{14} + \nu_{19} + \nu_{20})$$

It follows that

$$[\mathrm{H_2O_2}] = \frac{3.8 \times 10^6 \text{ cm}^{-3} \text{ sec}^{-1}}{\nu_{14} + \nu_{19} + \nu_{20}}$$

$$= \frac{3.8 \times 10^6 \text{cm}^{-3} \text{ sec}^{-1}}{2.4 \times 10^{-5} \text{ sec}^{-1}}$$

$$= 1.6 \times 10^{11} \text{ cm}^{-3}$$

$$\tau_{\mathrm{H_2O_2}} = (\nu_{14} + \nu_{19} + \nu_{20})^{-1}$$

$$= 4.2 \times 10^4 \text{ sec}$$

With our assumptions, the lifetime for H_2O_2 is about12 hours. ■

In calculating the abundance of H_2O_2 in Example 17.15, we assumed a balance between instantaneous (noon time) rates for production and loss; as indicated in Example 17.15; however, the lifetime of H_2O_2 is about 12 hours. It follows that the abundance of H_2O_2 should reflect not the instantaneous rates for production and loss but an average of these quantities over a period comparable to the lifetime of H_2O_2. Our analysis is deficient in another important respect: we allowed for production of HO_x by (17.6), but we did not explicitly account for the requirement that production of HO_x should be balanced by loss. With the simplified chemical scheme introduced here, accepting the indication that (17.14) and (17.20) provide the most important paths for removal of HO_x, it is apparent that the concentration of H_2O_2 must increase to the point where removal of HO_x by (17.14) and (17.20) should be sufficient to balance production by (17.6). To explore implications of these matters further, it is instructive to consider the evolution of HO_x chemistry with time from a hypothetical initial state in which concentrations of individual HO_x species are set equal to zero.

Let the clock begin ticking at midnight. According to our assumption, the abundance of HO_x species is initially zero and remains so until the sun rises and photolysis of O_3 initiates production of $O(^1D)$, OH, and HO_2 (recall that the lifetimes of OH and HO_2 are measured in seconds and minutes, respectively). Concentrations of OH and HO_2 build up during the morning responding to the increase in J_3 related to the decrease in solar zenith angle. They reach a maximum at noon, with values similar to those estimated in Examples 17.9 and 17.11. As rapidly as it is produced, HO_x is converted from OH to HO_2 and hence to H_2O_2. Reflecting cumulative production of HO_x by (17.6), H_2O_2 builds up. Assume a rate for production of OH over the course of the morning equal on average to half the value calculated for noon in Example 17.4. The total number of HO_x molecules formed between 6 A.M. and noon may be obtained by multiplying the average rate for production by the elapsed time (6 hours): $(3.9 \times 10^6\ cm^{-3}\ sec^{-1})$ $(2.2 \times 10^4\ sec) = 8.3 \times 10^{10}$ mol cm^{-3}, equivalent to 4.2×10^{10} mol cm^{-3} of H_2O_2 (recall that a molecule of H_2O_2 contains two molecules of HO_x). The number of H_2O_2 molecules produced over a 24-hour period is equal to approximately twice this value, $8.3 \times 10^{10}\ cm^{-3}$ (production of HO_x, is confined to the daylight hours: rates for photolysis of O_3, and consequently for the source of HO_x, should be symmetric with respect to noon). To balance the 24-hour source of HO_x, we require that the concentration of H_2O_2 rise to the point where removal of HO_x by (17.14) and (17.20) is sufficient over a 24-hour period to balance production by (17.6).

Example 17.16: Using the results developed above, calculate the concentration of H_2O_2, such that removal of HO_x by (17.14) and (17.20) should be sufficient to balance production by (17.6) for the surface at 30°N at equinox. As in Example 17.14, assume a rate constant for (17.20) of $2.3 \times 10^{-6}\ sec^{-1}$ equivalent to a lifetime for H_2O_2 of about five days. Assume an average loss frequency for (17.14) equal to 1/4 of the value used in Example 17.14, $\nu_{14} = 3.8 \times 10^{-6}\ sec^{-1}$, which is equivalent to assuming that the diurnally averaged concentration of OH is equal to 1/4 of the value calculated for noon.

Answer: According to the analysis above, reaction (17.6) contributes a source, S, of 1.7×10^{11} mol of HO_x over a 24-hour period (production is confined to the hours of daylight).

The instantaneous rate for loss of HO_x, $L(cm^{-3}\ sec^{-1})$, is equal to twice the rate for removal of H_2O_2 by (17.14) and (17.20):

$$L = 2\,[H_2O_2]\,(2.3 \times 10^{-6}\ sec^{-1} + 3.8 \times 10^{-6}\ sec^{-1})$$
$$= [H_2O_2]\,(1.2 \times 10^{-5}\ sec^{-1})$$

Thus, the total number (N) of HO_x molecules removed over a 24-hour period (loss can occur at night as well as during the day) is given by

$$N = L \times (8.6 \times 10^4\ sec)$$
$$= [H_2O_2] \times 1.03$$

Requiring that loss balance production implies that

$$S = N$$

or

$$[H_2O_2] = \frac{1.7 \times 10^{11}\ cm^{-3}}{1.03} = 1.7 \times 10^{11}\ cm^{-3}$$ ■

Returning now to our time-dependent scenario, the concentration of H_2O_2 will have risen at the end of day one to a level somewhat less than $8.5 \times 10^{10}\ cm^{-3}$ (not all of the H_2O_2 molecules produced will survive in the face of reactions 17.14 and 17.20). More than four days (several lifetimes) will be required to establish a steady state such that production of HO_x by (17.6) is balanced on average over a 24-period by removal due to (17.14) and (17.20).[6] The concentration of H_2O_2 will steadily increase over this period, rising towards the steady-state limit. Concentrations of OH and HO_2 will vary diurnally in response to changes in J_3. The amplitude of the diurnal cycle will increase as the system approaches steady state, reflecting production of OH associated with photolysis of H_2O_2.

Example 17.17: Repeat the calculation of [OH] outlined in Example 17.11, accounting for production of OH by photolysis of H_2O_2. Assume a concentration for H_2O_2 equal to the steady-state value derived in Example 17.16. Calculate the chain length for HO_x at noon allowing for the influence of (17.19).

Answer: The concentration of OH is given in this case by

$$[OH] = \frac{2k_6[O^1D][H_2O] + 2J_{19}[H_2O_2]}{k_{12}[CO] + k_{13}[CH_4]}$$

The rate for production by (17.19) is given by

$$2J_{19}[H_2O_2] = 2(6.5 \times 10^{-6}\ \text{sec}^{-1})(1.7 \times 10^{11}\ \text{cm}^{-3})$$
$$= 2.2 \times 10^{6}\ \text{cm}^{-3}\ \text{sec}^{-1}$$

Hence,

$$[OH] = \frac{(7.7 \times 10^{6} + 2.2 \times 10^{6})\ \text{cm}^{-3}\ \text{sec}^{-1}}{8.5 \times 10^{-1}\ \text{sec}^{-1}}$$
$$= 1.2 \times 10^{7}\ \text{cm}^{-3}$$

The chain length is

$$C = \frac{2k_6[O^1D][H_2O] + 2J_{19}[H_2O_2]}{2k_6[O^1D][H_2O]}$$
$$= \frac{(7.7 \times 10^{6} + 2.2 \times 10^{6})\ \text{cm}^{-3}\ \text{sec}^{-1}}{7.7 \times 10^{6}\ \text{cm}^{-3}\ \text{sec}^{-1}}$$
$$= 1.3$$

■

The discussion of HO_x chemistry presented here is intended to give the reader a feeling for numbers: the importance of the overlying column abundance of O_3 in regulating the primary source of HO_x; the sensitivity of HO_x to ambient levels of tropospheric O_3 and H_2O; the role of NO_x and O_3 in cycling HO_2 back to OH; and the need to allow for a full diurnal cycle in evaluating the overall balance of production and loss of HO_x. The treatment is deficient, however, in its neglect of secondary reactions involved in oxidation of CH_4. These reactions, as we shall see, can provide both sources and sinks for HO_x, the balance depending sensitively on the abundance of NO_x. We postpone a more complete discussion of HO_x chemistry until later, taking up now the chemistry of CO with an emphasis on the role of CO in the budget of tropospheric O_3.

17.2 The Chemistry of CO

Reaction (17.12) provides the primary sink for CO. The impact of CO on the budget of O_3 depends on the fate of HO_2 formed subsequently by (17.15). Allowing for the impact of CO on the overall budget of HO_x, we may identify three distinct sequences of reactions involved in oxidation of CO:

$$\begin{aligned} CO + OH &\rightarrow CO_2 + H \\ H + O_2 + M &\rightarrow HO_2 + M \\ NO + HO_2 &\rightarrow NO_2 + OH \\ h\nu + NO_2 &\rightarrow NO + O \\ O + O_2 + M &\rightarrow O_3 + M, \end{aligned} \qquad (17.27)$$

$$\begin{aligned} CO + OH &\rightarrow CO_2 + H \\ H + O_2 + M &\rightarrow HO_2 + M \\ HO_2 + O_3 &\rightarrow OH + 2O_2, \end{aligned} \qquad (17.28)$$

and

$$\begin{aligned} h\nu + O_3 &\rightarrow O(^1D) + O_2 \\ O(^1D) + H_2O &\rightarrow 2OH \\ 2[CO + OH &\rightarrow CO_2 + H] \\ 2[H + O_2 + M &\rightarrow HO_2 + M] \\ 2HO_2 &\rightarrow H_2O_2 + O_2 \\ H_2O_2 &\rightarrow \text{products} \end{aligned} \qquad (17.29)$$

Sequence (17.27) implies net production of O_3, as summarized by (17.1). Ozone is removed in (17.28) and (17.29). The net reaction for (17.28) is equivalent to (17.2), and the sequence (17.29) is equivalent to:

$$2CO + O_3 + H_2O \rightarrow 2CO_2 + H_2O_2 \text{ products} \qquad (17.30)$$

The critical step in the production of O_3 in (17.27) involves the reaction of NO with HO_2, reaction (17.16). It is convenient here, as it was for the stratosphere, to draw on the concept of odd oxygen, defined for present purposes as the combination of O_3, O, $O(^1D)$, and NO_2.[7] Reaction (17.16) provides the primary source for tropospheric odd oxygen. It is removed by a combination of (17.6), (17.17), (17.21), and

$$OH + O_3 \rightarrow HO_2 + O_2 \qquad (17.31)$$

The rate at which odd oxygen, and consequently O_3, is produced by (17.16) is given by

$$p(O_3) = k_{16}\,[NO][HO_2] \qquad (17.32)$$

If we assume that HO_x is removed by a combination of (17.14) and (17.20), the HO_x balance may be expressed in terms of the source-sink relation

$$2k_6\,[O^1D][H_2O] = 2\epsilon k_{18}\,[HO_2]^2, \qquad (17.33)$$

where ϵ defines the probability that H_2O_2 is lost by the combination of the HO_x sink reactions (17.14) and (17.20), rather than by (17.19).[8] Using (17.10) to substitute for $[O^1D]$,

$$\frac{2k_6 J_3 f_{H_2O}[O_3]}{k^*} = 2\epsilon k_{18}\,[HO_2]^2 \qquad (17.34)$$

It follows that

$$[HO_2] = \left(\frac{k_6 J_3 f_{H_2O}[O_3]}{\epsilon k^* k_{18}}\right)^{1/2}, \qquad (17.35)$$

and the rate for production of O_3, (17.32), is given by

$$p(O_3) = k_{16}\,[NO]\left(\frac{k_6 J_3 f_{H_2O}[O_3]}{\epsilon k^* k_{18}}\right)^{1/2} \qquad (17.36)$$

Assume that (17.6) provides the dominant loss mechanism for odd oxygen. It follows that the rate for production of O_3 will exceed the rate of loss if

$$k_{16}\,[NO][HO_2] > k_6\,[O(^1D)][H_2O] \qquad (17.37)$$

Using (17.35) and (17.10) to substitute for $[HO_2]$ and $[O(^1D)]$, this inequality may be recast in the form

$$[\mathrm{NO}] > \frac{1}{k_{16}}\left(\frac{k_6 J_3 \epsilon k_{18}}{k^*} f_{H_2O}[O_3]\right)^{1/2} \qquad (17.38)$$

Reversing the direction of the inequality sign defines the condition under which loss of O_3 dominates production.

Example 17.18: Estimate, for the surface at 30°N, for noon at equinox, the concentration of NO for which production of odd oxygen by (17.16) is comparable to loss by (17.6). As in Example 17.4, assume a value for J_3 of 2.4×10^{-5} sec^{-1}, with mixing ratios of H_2O and O_3 equal to 1.7×10^{-2} and 5×10^{-8}, respectively. Values for other rate constants may be taken from the data included in Table 17.1. The value of ϵ may be taken equal to 1.

Answer: The concentration of NO at which rates of production and loss of odd oxygen are in balance is given by replacing the inequality sign in (17.38) with an equality:

$$[\mathrm{NO}] = \frac{1}{k_{16}}\left\{\frac{k_6 J_3 \epsilon k_{18}}{k^*}\right\}^{1/2} f_{H_2O}^{1/2}[O_3]^{1/2}$$

Assuming a mixing ratio for O_3 of 5×10^{-8} with a total density [M] of 2.5×10^{19} cm^{-3}:

$$[O_3] = 5 \times 10^{-8} \times 2.5 \times 10^{19} \text{ cm}^{-3}$$
$$= 1.25 \times 10^{11} \text{ cm}^{-3}$$

Substituting for the various rate constants and for f_{H_2O} and $[O_3]$, omitting units (all quantities are expressed in the *cgs* convention),

$$[\mathrm{NO}] = \frac{1}{8.7 \times 10^{-12}} \times \left[\frac{(2.2 \times 10^{-10})(2.4 \times 10^{-5})(3.1 \times 10^{-12})}{3 \times 10^{-11}}\right]^{1/2} \times [(1.7 \times 10^{-2})(1.25 \times 10^{12})]^{1/2}$$
$$= 3.9 \times 10^8 \text{ cm}^{-3}$$

This corresponds to a mixing ratio for NO of

$$f_{NO} = \frac{3.9 \times 10^8}{(2.5 \times 10^{19})} = 1.6 \times 10^{-11}$$

It follows that oxidation of CO may be expected to result in net production of O_3 if the mixing ratio of NO is greater than about 16 ppt. ■

Example 17.19: Assuming that the relative abundances of NO and NO_2 are determined by a balance of

$$\mathrm{NO} + O_3 \rightarrow \mathrm{NO_2} + O_2 \qquad (17.39)$$

and

$$h\nu + \mathrm{NO_2} \rightarrow \mathrm{NO} + O, \qquad (17.40)$$

estimate the value of $[NO_2]$, and thus the abundance of NO_x, corresponding to the concentration of NO derived in Example 17.18. Assume rate constants for (17.39) and (17.40) of 1.7×10^{-14} cm^3 sec^{-1} and 7.9×10^{-3} sec^{-1}, respectively.

Answer: Equating production and loss of NO_2:

$$k_{39}[\mathrm{NO}][O_3] = J_{40}[\mathrm{NO_2}],$$

where k_{39} and J_{40} define the rate constants for (17.39) and (17.40), respectively.

Thus,

$$\frac{[\mathrm{NO}]}{[\mathrm{NO_2}]} = \frac{J_{40}}{k_{39}[O_3]}$$

Omitting units as before,

$$\frac{[\mathrm{NO}]}{[\mathrm{NO_2}]} = \frac{7.9 \times 10^{-3}}{(1.7 \times 10^{-14})(1.3 \times 10^{12})}$$

Hence,

$$[\mathrm{NO_2}] = 1.1 \times 10^9 \text{ cm}^{-3}$$

The abundance of NO_x is given by

$$[\mathrm{NO_x}] = [\mathrm{NO}] + [\mathrm{NO_2}] = 1.5 \times 10^9 \text{ cm}^{-3},$$

corresponding to a mixing ratio, f_{NO_x}, of 60 ppt. ■

Example 17.19 indicates that NO_2 is the dominant form of NO_x, even at noon. The abundance of NO is directly proportional to the abundance of NO_2 (and consequently NO_x) and inversely proportional to the abundance of O_3:

$$[\mathrm{NO}] = \frac{J_{40}[\mathrm{NO_2}]}{k_{39}[O_3]} \qquad (17.41)$$

It follows, substituting for NO in (17.36), that production of O_3 is proportional to the abundance of NO_x and inversely proportional to the square root of the concentration of O_3:

$$p(O_3) \sim \frac{f_{NO_x}}{f_{O_3}^{1/2}} \qquad (17.42)$$

As indicated by the analysis leading to (17.38), the transition between net loss and net production of O_3 takes place at a concentration of NO_2 (the dominant form of NO_x) given by

$$[\mathrm{NO_2}] = \frac{k_{39}}{J_{40}k_{16}}\left\{\frac{k_6 J_3 \epsilon k_{18}}{k^*}\right\}^{1/2}[f_{H_2O}]^{1/2}[O_3]^{3/2} \qquad (17.43)$$

The crossover corresponds to the situation where the rate for reaction (17.16) is comparable to that for (17.18). For concentrations of NO_2 less than the value given by (17.43), cycling of HO_x from HO_2 to OH is unimportant: the chemistry of HO_x involves a unidirectional flow of HO_x from OH to HO_2

to H_2O_2; oxidation of CO is associated with net loss of O_3. For concentrations of NO_2 larger than (17.43), cycling of HO_x between HO_2 and OH (by reactions 17.12 and 17.16) is significant. Odd oxygen is produced each time the cycle is traversed and oxidation of CO results in net production of O_3.

We assumed in the analysis to this point that HO_x is removed mainly as H_2O_2, either by (17.14) or by (17.20): this condition served to fix the concentration of HO_2 as indicated in equation (17.35). For high concentrations of NO_x, we must allow for the removal of HO_x in the form of HNO_3 produced by reaction (17.21). Under conditions where HNO_3 rather than H_2O_2 provides the dominant sink for HO_x, the HO_x balance is given by

$$2k_6\,[O^1D][H_2O] = k_{21}\,[OH][NO_2][M] \qquad (17.44)$$

As we have seen, cycling of HO_x by (17.12) and (17.16) results in production of O_3 and is rapid at high concentrations of NO_x:

$$p(O_3) = k_{12}\,[OH][CO] = k_{16}\,[HO_2][NO] \qquad (17.45)$$

Using (17.44) to substitute for [OH] in (17.45), with $[O^1D]$ given by (17.10), we find

$$p(O_3) = \frac{2k_{12}k_6J_3}{k^*k_{21}} f_{O_3} f_{H_2O} \frac{[CO]}{[NO_2]} \qquad (17.46)$$

It follows, for high concentrations of NO_x, that the rate for production of O_3 is proportional to the abundance of CO and inversely proportional to the abundance of NO_x. The inverse relationship between $p(O_3)$ and $[NO_x]$ reflects the fact that at high NO_x the concentration of OH is fixed by the abundance of NO_x; the larger the abundance of NO_x, the lower the abundance of OH and as a consequence the slower the rate for production of O_3.

Example 17.20: Estimate for 30°N, at equinox and at noon, the concentration of NO_x at which we might expect the switchover to occur from H_2O_2 to HNO_3 control of HO_x. Assume concentrations of O_3, H_2O, and other quantities, as used in the preceding examples.

Answer: The switchover corresponds approximately to the point at which the rate for removal of HO_x in the HO_x–only scheme, mainly by (17.14), is equal to the rate for removal by (17.21):

$$2k_{14}\,[OH][H_2O_2] = k_{21}\,[OH][NO_2][M],$$

where k_{21} denotes the rate constant for (17.21). The factor of two reflects the fact that two molecules of HO_x are removed by (17.14). It follows that

$$[NO_2] = \frac{2k_{14}[H_2O_2]}{k_{21}[M]}$$

Using the concentration of H_2O_2 obtained in Example 17.16,

$$[NO_2] = \frac{2(1.7\times10^{-12}\ \text{cm}^3\ \text{sec}^{-1})(1.7\times10^{11}\ \text{cm}^{-3})}{(4.8\times10^{-31}\ \text{cm}^6\ \text{sec}^{-1})(2.5\times10^{19}\ \text{cm}^{-3})}$$

$$= 5\times10^{10}\ \text{cm}^{-3}$$ ■

The value of $[NO_2]$ obtained in Example 17.20 corresponds to a NO_x mixing ratio of about 3 ppb. In practice, the concentration of NO_x at the transition point, estimated in this fashion, is a little high: a more complete analysis locates the transition at a NO_x mixing ratio closer to 1 ppb. The discrepancy reflects the assumption that the concentration of H_2O_2 was taken equal to the value derived in Example 17.16. At high concentrations of NO_x, however, the abundance of HO_2 is reduced and production of H_2O_2 is suppressed relative to the value assumed in Example 17.16. It would have been more appropriate here to have used a concentration of H_2O_2 of about 6×10^{10} cm^{-3}.

As indicated in (17.42), the rate for production of O_3 is proportional to the NO_x mixing ratio when the concentration of NO_x is small. For high concentrations of NO_x, it varies inversely as the mixing ratio of NO_x. Detailed calculations, summarized in Figures 17.7 and 17.8, indicate that production of O_3 is a maximum for a concentration of NO_x equal to about 1 ppb.

A slightly different view of O_3 production is presented in Figure 17.9, which shows the response to a combination of emissions of CO and NO_x. We assumed in this analysis that emissions were confined to a thin layer, 500 m thick, near the surface as would arise if the lowest region of the atmosphere was capped by a strong inversion, a common occurrence in cities such as Los Angeles. The results presented here suggest that, if the source of NO_x was less than about 5×10^{10} cm^{-2} sec^{-1}, a reduction in NO_x emissions would lead to a lower rate for production of O_3. If the source of NO_x was larger than 5×10^{10} cm^{-2} sec^{-1}, a drop in NO_x emissions could result in an *increase* in O_3. Production of O_3 is rela-

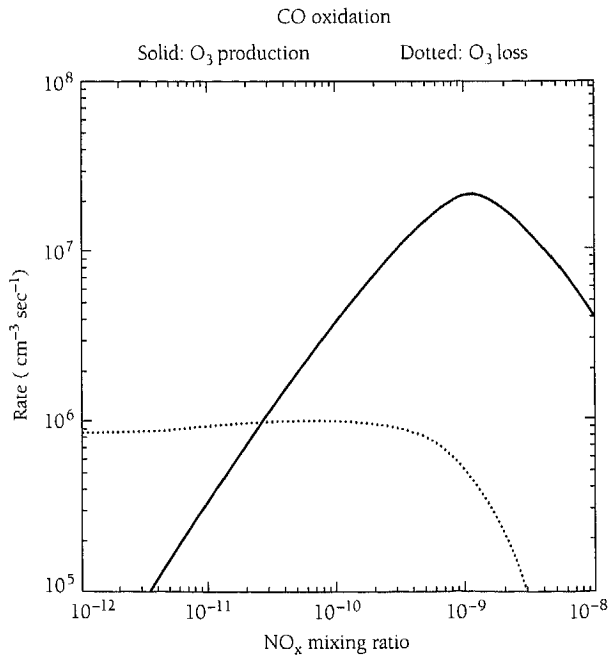

Figure 17.7 Ozone production (solid line) from reaction (17.16) and ozone loss (dotted line) due to reaction (17.17), as a function of NO_x. Values are calculated near the surface at 30°N for equinoctial conditions.

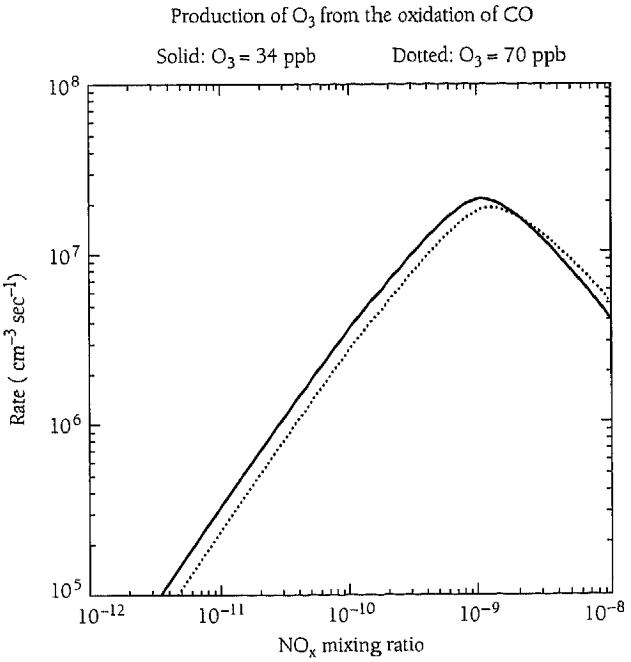

Figure 17.8 Ozone production from reaction (17.16) as a function of NO_x with fixed background mixing ratios of ozone of 34 ppb (solid line) and 70 ppb (dotted line). Values are calculated near the surface at 30°N for equinoctial conditions.

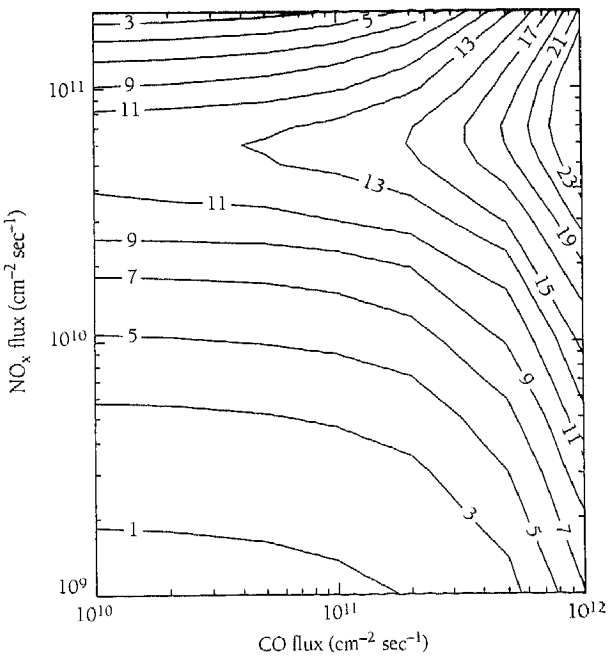

Figure 17.9 Ozone production [in units of $10^6 cm^{-3} sec^{-1}$ from reaction (17.16)] as a function of emission of NO_x and CO. Results are given for 30°N at equinox, with the assumption that the emissions are confined to a 0.5 km layer above the surface.

tively insensitive to emission of CO if the source strength is less than about 10^{11} cm^{-2} sec^{-1} (as indicated by the relatively flat shape of the contours on the left-hand side of Figure 17.9). If emission rates for NO_x and CO are both high (corresponding to the upper right-hand side of Figure 17.9), a reduction in the source of O_3 could be accomplished either by a *decrease* in emissions of CO or by an *increase* in emissions of NO_x.

The behavior illustrated in Figures 17.7–17.9 poses an interesting dilemma for policy makers concerned with regulation of emissions to reduce the buildup of O_3. It suggests that if mixing ratios of NO_x were larger than about 1 ppb (emission rates higher than 5×10^{10} cm^{-2} sec^{-1} in Figure 17.9), a reduction in O_3 could be brought about by an *increase* in emissions of NO_x. This could be interpreted as a license to pollute. The decrease in the rate of production of O_3 at high concentrations of NO_x reflects the role of (17.21) as a sink for OH. The concentration of OH is suppressed, resulting in a decrease in the rate of oxidation of CO.

17.3 The Chemistry of CH_4

The sequence of reactions implicated in oxidation of CH_4 is significantly more complex than that involved in oxidation of CO. As with CO, the sequence is initiated by reaction with OH:

$$OH + CH_4 \rightarrow H_2O + CH_3 \qquad (17.47)$$

The methyl radical (CH_3) formed in (17.47) combines with O_2 to produce the methylperoxy radical (CH_3O_2):

$$CH_3 + O_2 + M \rightarrow CH_3O_2 + M \qquad (17.48)$$

We can think of the methyl radical formed by (17.47) as analogous to the H atom produced when OH reacts with CO, reaction (17.12). The methylperoxy radical formed in (17.48) is chemically similar to the hydroperoxy radical (HO_2) produced in (17.15). As was the case for HO_2, the subsequent chemistry depends on the supply of NO. It is convenient to distinguish from the outset between the low and high NO_x environments.

In the low-NO_x regime, CH_3O_2 is initially converted to methylhydroperoxide (CH_3OOH) by reaction with HO_2:

$$CH_3O_2 + HO_2 \rightarrow CH_3OOH + O_2 \qquad (17.49)$$

Reaction (17.49) is analogous to (17.18), which is responsible for production of H_2O_2. Subsequent reactions, either

$$CH_3OOH + OH \rightarrow CH_2O + OH + H_2O \qquad (17.50)$$

or

$$CH_3OOH + h\nu \rightarrow CH_3O + OH$$

and

$$CH_3O + O_2 \rightarrow CH_2O + HO_2, \qquad (17.51)$$

result in conversion of CH_3OOH to formaldehyde (CH_2O). Sequence (17.47), followed by (17.48), (17.49), and (17.50), is equivalent to

$$OH + HO_2 + CH_4 \rightarrow 2H_2O + CH_2O \qquad (17.52)$$

Reaction (17.47), followed by (17.48), (17.49), and (17.51), is equivalent to

$$CH_4 + O_2 \rightarrow CH_2O + H_2O \qquad (17.53)$$

The radicals OH and HO_2 consumed in (17.52) may be supplied by (17.6), followed by

$$OH + O_3 \rightarrow HO_2 + O_2 \qquad (17.54)$$

Accounting for (17.3), (17.6), and (17.54), (17.52) may be written in the summary form

$$CH_4 + 2O_3 \rightarrow CH_2O + H_2O + 2O_2 \qquad (17.55)$$

Reactions (17.53) and (17.55) summarize alternate paths in the low-NO_x regime for what may be considered the first stage in the oxidation of CH_4. The oxidation state of carbon is raised by four units in the transition from CH_4 (−4) to CH_2O (0). We shall refer to the sequence of reactions involved in (17.53) and (17.55) as *Ia* and *Ib*, respectively. Molecular oxygen serves as the oxidant for Ia. The oxidant for Ib is O_3: two moles of O_3 are consumed by Ib for every mole of CH_4 converted to CH_2O in Ib. The specific reactions involved in these sequences are summarized in Table 17.2.

Formaldehyde may be removed by photolysis, either by

$$h\nu + CH_2O \rightarrow CO + H_2 \qquad (17.56)$$

or by

$$h\nu + CH_2O \rightarrow CHO + H, \qquad (17.57)$$

with the H atom in (17.57) converted to HO_2 by (17.15). Reaction with OH provides an additional sink:

$$OH + CH_2O \rightarrow CHO + H_2O \qquad (17.58)$$

The CHO radical reacts rapidly with O_2 to form CO and HO_2:

$$CHO + O_2 \rightarrow CO + HO_2 \qquad (17.59)$$

Molecular hydrogen formed by (17.56) is removed by reaction with OH, forming H_2O:

$$OH + H_2 \rightarrow H_2O + H, \qquad (17.60)$$

with the H atom in (17.60) subsequently converted to HO_2 by (17.15). Sequence (17.3), followed by (17.6), (17.56), (17.60), and (17.15), is equivalent to

$$CH_2O + O_3 \rightarrow CO + OH + HO_2 \qquad (17.61)$$

Reaction (17.57), followed by (17.15) and (17.59), is equivalent to

$$CH_2O + 2O_2 \rightarrow CO + 2HO_2, \qquad (17.62)$$

while (17.1), followed by (17.6), (17.58), and (17.59), corresponds to

$$CH_2O + O_3 \rightarrow CO + OH + HO_2 \qquad (17.63)$$

We shall refer to the sequences of reactions involved in oxidation of CH_2O to CO, (17.61), (17.62), and (17.63), as IIa, IIb, and IIc. The elementary reactions involved in these sequences are summarized in Table 17.3.

Table 17.2 Sequences of Reactions Involved in the Oxidation of CH_4 to CH_2O

Sequence Ia (low NO_x)
$OH + CH_4 \rightarrow H_2O + CH_3$
$CH_3 + O_2 + M \rightarrow CH_3O_2 + M$
$CH_3O_2 + HO_2 \rightarrow CH_3OOH + O_2$
$CH_3OOH + h\nu \rightarrow CH_3O + OH$
$CH_3O + O_2 \rightarrow CH_2O + HO_2$
Net: $CH_4 + O_2 \rightarrow CH_2O + H_2O$
Sequence Ib (low NO_x)
$h\nu + O_3 \rightarrow O(^1D) + O_2$
$O(^1D) + H_2O \rightarrow OH + OH$
$OH + O_3 \rightarrow HO_2 + O_2$
$OH + CH_4 \rightarrow H_2O + CH_3$
$CH_3 + O_2 + M \rightarrow CH_3O_2 + M$
$CH_3O_2 + HO_2 \rightarrow CH_3OOH + O_2$
$CH_3OOH + OH \rightarrow CH_2O + OH + H_2O$
Net: $CH_4 + 2O_3 \rightarrow CH_2O + H_2O + 2O_2$
Sequence Ic (high NO_x)
$OH + CH_4 \rightarrow H_2O + CH_3$
$CH_3 + O_2 + M \rightarrow CH_3O_2 + M$
$CH_3O_2 + NO \rightarrow CH_3O + NO_2$
$CH_3O + O_2 \rightarrow CH_2O + HO_2$
$HO_2 + NO \rightarrow OH + NO_2$
$2\ \{h\nu + NO_2 \rightarrow NO + O\}$
$2\ \{O + O_2 + M \rightarrow O_3 + M\}$
Net: $CH_4 + 4O_2 \rightarrow CH_2O + 2O_3 + H_2O$

Table 17.3 Sequences of Reactions Involved in the Oxidation of CH_2O to CO

Sequence IIa
$h\nu + O_3 \rightarrow O(^1D) + O_2$
$O(^1D) + H_2O \rightarrow OH + OH$
$h\nu + CH_2O \rightarrow CO + H_2$
$OH + H_2 \rightarrow H_2O + H$
$H + O_2 + M \rightarrow HO_2 + M$
Net: $CH_2O + O_3 \rightarrow CO + OH + HO_2$
Sequence IIb
$h\nu + CH_2O \rightarrow CHO + H$
$H + O_2 + M \rightarrow HO_2 + M$
$CHO + O_2 \rightarrow CO + HO_2$
Net: $CH_2O + 2O_2 \rightarrow CO + 2HO_2$
Sequence IIc
$h\nu + O_3 \rightarrow O(^1D) + O_2$
$O(^1D) + H_2O \rightarrow OH + OH$
$OH + CH_2O \rightarrow CHO + H_2O$
$CHO + O_2 \rightarrow CO + HO_2$
Net: $CH_2O + O_3 \rightarrow CO + OH + HO_2$

Oxidation of CH_4 is completed by reaction of CO with OH, (17.12). If the abundance of NO_x is low, such that reactions involving NO may be ignored, we see that oxidation of CH_4 is generally responsible for a net loss of O_3. Depending on the details of the reaction path, as many as three or as few as zero molecules of O_3 may be consumed in the oxidation of CH_4 to CO_2 in the absence of NO_x. The sequence Ib followed by IIa, (17.12) and (17.15), for example, is equivalent to

$$CH_4 + 3O_3 \rightarrow CO_2 + H_2O + 2HO_2 + O_2 \quad (17.64)$$

On the other hand, Ia, followed by IIc, (17.12), and (17.15), is equivalent to

$$CH_4 + O_3 + 2O_2 \rightarrow CO_2 + 2HO_2 + H_2O \quad (17.65)$$

The key difference between the path for oxidation of CH_4 in the presence and absence of NO_x concerns the fate of the peroxy radicals HO_2 and CH_3O_2. Given an adequate source of NO_x, these radicals are removed by reaction with NO resulting in a sequence of reactions leading to production of O_3:

$$\begin{aligned} RO_2 + NO &\rightarrow RO + NO_2 \\ h\nu + NO_2 &\rightarrow NO + O \\ O + O_2 + M &\rightarrow O_3 + M \end{aligned} \quad (17.66)$$

Here R denotes either H or CH_3. Oxidation of CH_4 to CH_2O proceeds in this case by a suite of reactions indicated as sequence Ic in Table 17.2. Sequence Ic leads to production of two molecules of O_3 for each molecule of CH_4 converted to CH_2O through the reaction sequence summarized by

$$CH_4 + 4O_2 \rightarrow CH_2O + 2O_3 + H_2O \quad (17.67)$$

Sequence Ic, followed by IIb and (17.27), is equivalent to

$$CH_4 + 8O_2 \rightarrow CO_2 + 3O_3 + 2HO_2 + H_2O \quad (17.68)$$

If we assume that the HO_2 radicals produced in (17.68) are converted to OH by (17.66), we see that oxidation of a single molecule of CH_4 in the presence of NO_x can account for the production of as many as five molecules of O_3 and two molecules of OH:

$$CH_4 + 10O_2 \rightarrow CO_2 + 5O_3 + 2OH + H_2O \quad (17.69)$$

Reaction (17.69) provides an example of what is known as a **chain mechanism** for production of O_3. The chain is *initiated* by (17.6). It is *propagated* by the complex suite of reactions outlined above. It is *terminated* when radicals are removed by reactions such as (17.20) and (17.21). In the presence of NO_x, oxidation of CH_4 is sustained by a sequence of reactions catalyzed by HO_x and NO_x. In the absence of NO_x, oxidation of CH_4 (and other hydrocarbons) in the troposphere would be limited by supply of O_3 from the stratosphere. A diagrammatic representation of the key steps involved in oxidation of CH_4 is presented in Figure 17.10.

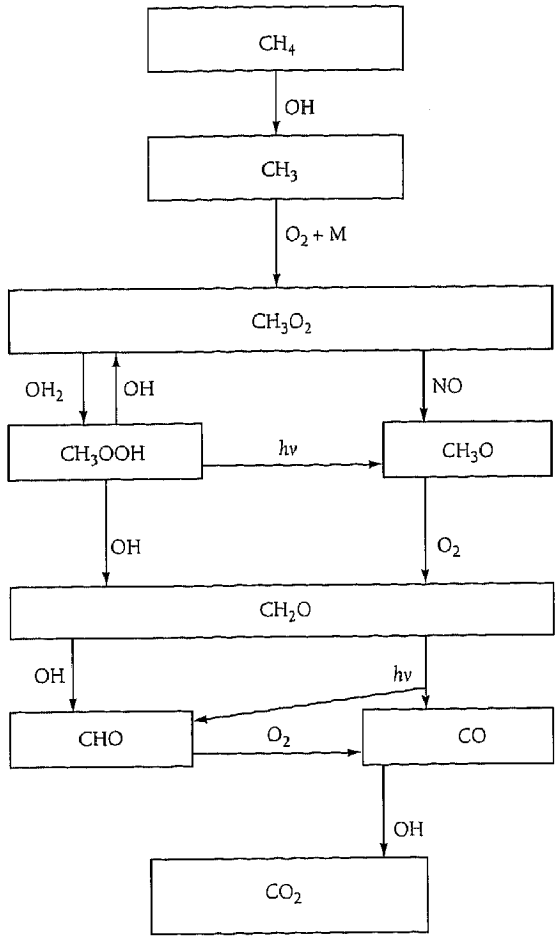

Figure 17.10 The reaction pathway for the oxidation of CH_4 to CO_2. Source: Logan et al. 1981.

17.4 The Chemistry of Smog

We turn our attention now to the chemistry of polluted environments. Specifically, we explore the conditions that lead to production of high levels of O_3 in urban and regional environments subject to high emission rates of anthropogenic hydrocarbons and NO_x.

As was seen for CH_4, oxidation of hydrocarbons is initiated by reaction with OH. Denoting a representative hydrocarbon as *RH*, where *R* denotes an organic group, the first step in oxidation is given by

$$RH + OH \rightarrow R + H_2O \quad (17.70)$$

This is followed by formation of a peroxy radical (analogous to the production of CH_3O_2 in the oxidation of CH_4):

$$R + O_2 + M \rightarrow RO_2 + M \quad (17.71)$$

Ozone is produced subsequently by

$$RO_2 + NO \rightarrow HO_2 + \begin{pmatrix} \text{aldehyde} \\ \text{or} \\ \text{carbonyl} \end{pmatrix} + NO_2, \quad (17.72)$$

$$HO_2 + NO \rightarrow OH + NO_2, \quad (17.73)$$

and

$$2\{NO_2 + h\nu \rightarrow NO + O\}, \quad (17.74)$$

followed by

$$2\{O + O_2 + M \rightarrow O_3 + M\} \qquad (17.75)$$

The sequence (17.70)–(17.75), essentially a generalization of Ic presented in Table 17.2 for CH_4, is equivalent to

$$RH + 3O_2 \rightarrow \begin{pmatrix} \text{aldehyde} \\ \text{or} \\ \text{carbonyl} \end{pmatrix} + 2O_3 + H_2O \qquad (17.76)$$

Reactions (17.70)–(17.75) provide an example of what we referred to above as a *chain mechanism* for production of O_3. The chain is initiated by production of OH (by reaction 17.6 for example); production of O_3 is catalyzed during chain propagation by HO_x and NO_x; the chain is terminated by reactions resulting in removal of either HO_x or NO_x. The key reactions involved in chain termination are (17.18) and (17.21). Reaction (17.18) dominates when the abundance of NO_x is low; reaction (17.21) is more important when the abundance of NO_x is high.

Noting that the key (or rate-limiting) steps for production of O_3 by (17.70)–(17.75) are represented by (17.72) and (17.73) and that the rates (cm^{-3} sec^{-1}) for these reactions must be equal (they occur as part of a sequence), the rate for production of O_3, P_{O_3}, may be written as either twice the rate for (17.72) or twice the rate for (17.73). Following the earlier discussion of the production of O_3 by oxidation of CO (Section 17.2), we choose to write P_{O_3} in the form

$$P_{O_3} = 2\,k_{73}\,[NO][HO_2] \qquad (17.77)$$

In the low-NO_x regime, where HO_x is removed mainly by (17.18), followed by (17.14) or (17.20), it follows (see argument leading up to the derivation of 17.33) that

$$P_{HO_x} = 2\,\epsilon k_{18}\,[HO_2]^2 \qquad (17.78)$$

Here P_{HOx} denotes the rate for production of HO_x. Using (17.78) to substitute for $[HO_2]$ in (17.77), the rate for production of O_3 is given by

$$P_{O_3} = 2\,k_{73}\left(\frac{P_{HO_x}}{2\epsilon k_{18}}\right)^{1/2}[NO] \qquad (17.79)$$

In the high-NO_x regime, where HO_x is removed mainly by (17.21), the HO_x budget is determined by

$$P_{HO_x} = k_{21}\,[OH][NO_2][M] \qquad (17.80)$$

It follows that

$$[OH] = \frac{P_{HO_x}}{k_{21}[NO_2][M]} \qquad (17.81)$$

The production rate of O_3 equals twice the rate for reaction (17.70):

$$P_{O_3} = 2\,k_{70}\,[OH][RH] \qquad (17.82)$$

Using (17.81) to substitute for OH in (17.82), the rate for production of O_3 in the high-NO_x regime is given by

$$P_{O_3} = \frac{2k_{70}P_{HO_x}[RH]}{k_{21}[NO_2][M]} \qquad (17.83)$$

As we have seen, production of O_3 depends on the rate of reaction (17.16). Thus it is proportional to the product of the concentrations of NO and HO_2. The abundance of HO_2 is independent of the abundances of both NO_x and hydrocarbons in the low-NO_x regime. It is determined by a balance between production of HO_x by (17.6) (accounting for additional production as a byproduct of the oxidation chain) and removal by (17.18). At low levels of NO_x, therefore, production of O_3 is proportional to the abundance of NO_x and independent of the abundance of hydrocarbons. Conditions for production of O_3 in this regime are said to be **NO_x limited**. At higher levels of NO_x, production of HO_x is balanced mainly by (17.21). In this case the concentration of OH varies inversely as the concentration of NO_x. The concentration of OH is independent of the concentration of hydrocarbons at high levels of NO_x. An increase in supply of hydrocarbons results in a proportional increase in production of O_3. In this sense, production of O_3 at high levels of NO_x is said to be **hydrocarbon limited**.

The distinction between the high- and low-NO_x regimes is clearly illustrated in Figure 17.11. The Figure indicates concentrations of O_3 expected to develop under summer conditions in the United States as a result of specified rates for emission of NO_x and industrial hydrocarbons. The model used to derive these results allowed for the presence

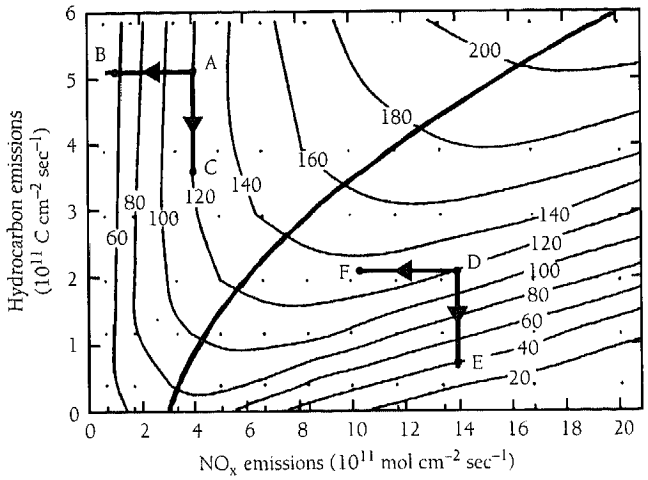

Figure 17.11 Isolines of ozone (in ppb) as a function of NO_x and anthropocentric hydrocarbon emission rates. Results of a two-layer model are shown for 1600 LT on the fourth day. The dots indicate emission rates of NO_x and hydrocarbons for individual simulations. The thick line running from the bottom left to the top right indicates the boundary between NO_x-limited and hydrocarbon-limited regimes. The arrows show successful and futile emissions control choices in each regime. In the NO_x-limited regime, reducing NO_x emissions greatly decreases ambient O_3 concentrations (A→B), while decreasing hydrocarbon emissions have no effect on air quality (A→C). In the hydrocarbon-limited regime, reducing hydrocarbon emissions decreased ambient O_3 concentrations (D→E), while decreasing NO_x emissions actually increases the ambient O_3 concentrations (D→F). Implementing the wrong control strategy might thus have no effect, or even an adverse effect. Source: Sillman, Logan, and Wofsy 1990.

of a boundary layer near the surface in which it was assumed that the atmosphere was efficiently mixed by convective processes during the day. The boundary layer climbed from about 100 m in early morning, extending to about 1800 m during late afternoon, and dropping to the surface at night. It was assumed that these relatively stable conditions persisted for four days. The results in Figure 17.11 refer to 1600 hours local time (LT) on Day 4.

The boundary between NO_x- and hydrocarbon-limiting conditions is approximately indicated by the solid line extending from the bottom left to the upper right-hand of Figure 17.11. Note that above the line, in the NO_x-limited condition, concentrations of O_3 are essentially independent of the magnitude of the source of hydrocarbons. A reduction in input of hydrocarbons, from 5.2×10^{11} to 3.5×10^{11} C atoms cm^{-2} sec^{-1} (as indicated by the segment A→C), leads to no net change in O_3. In contrast, a decrease in emissions of NO_x from 4×10^{11} to 1×10^{11} mol cm^{-2} sec^{-1} (as indicated by A→B), would result in a decrease in O_3 of more than 60 ppb, from 120 to less than 60 ppb. Quite different behavior is observed below the line, in the hydrocarbon-limited regime. A decrease of NO_x from 14×10^{11} to 10×10^{11} mol cm^{-2} sec^{-1} (as indicated by D→F) would result in a small increase in O_3, from 120 ppb to about 130 ppb. Clearly, efforts to improve air quality in the hydrocarbon-limited regime would be better served by working to reduce emissions of hydrocarbons. A reduction in hydrocarbon emissions from 2.2×10^{11} to 0.8×10^{11} C atoms cm^{-2} sec^{-1} (as indicated by the D→E segment) would provide for a reduction in O_3 of about 80 ppb, from 120 to about 40 ppb.

The results in Figure 17.11 considered the effects of emissions of NO_x and *anthropogenic* sources of hydrocarbons; a more realistic simulation should allow additionally for the impact of *natural* sources of hydrocarbons. Of particular importance in this context is emission of isoprene (CH_2=CH-C(CH_3)=CH_2), released as a by-product of photosynthesis. Figure 17.12 summarizes the results of a study designed to simulate production of O_3 over the eastern United States under hot, stagnant conditions characteristic of situations arising several times over the course of a typical summer.

Results in Figure 17.12a refer to an air mass originating on Day 1 in Illinois, moving over Indiana, Ohio, and Pennsylvania and reaching New York four days later. Figure 17.12b refers to a trajectory beginning in Missouri, crossing the Ohio River Valley, and arriving in West Virginia on Day 4. The model considered meteorological conditions typical of environments observed to result in the buildup of unhealthy levels of O_3. It assumed a wind speed of 3 m sec^{-1}, temperatures averaging about 298K, and a boundary layer reaching to a height of about 1500 m in the atmosphere during late afternoon. Emissions of NO_x and anthropogenic hydrocarbons were taken from the National Acid Precipitation Assessment Program (NAPAP) and were selected to represent typical midweek conditions for the region during summer. Emissions of isoprene were calculated using procedures described by Lamb et al. (1987) and accounting for regional

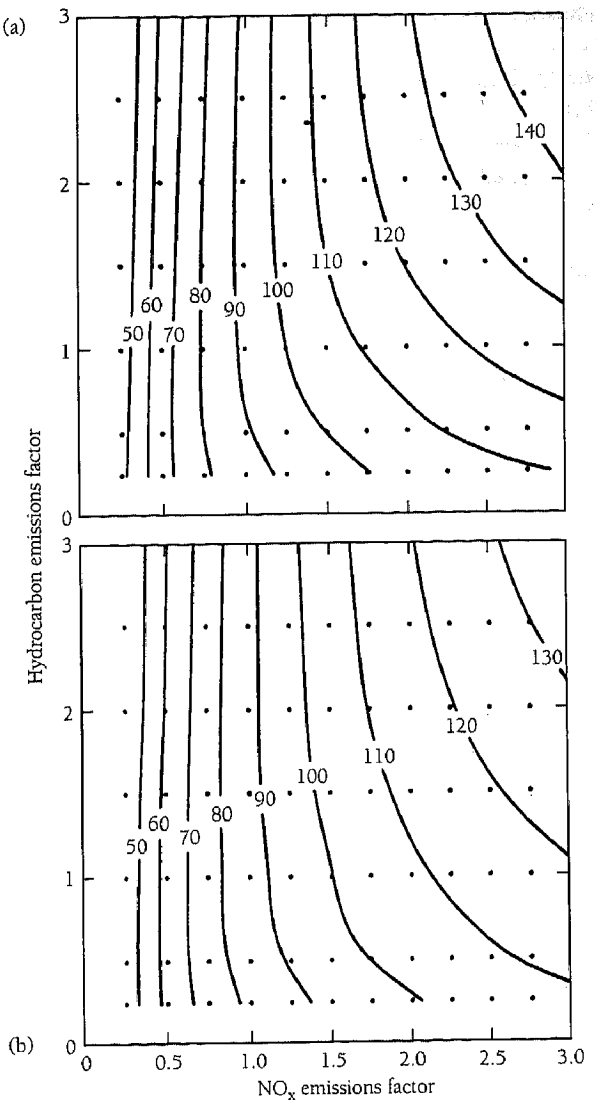

Figure 17.12 Ozone (in ppb) in rural U.S.A., as a function of NO_x and hydrocarbon emissions. The top panel (a) shows results for New York for an air mass that originated four days earlier in Illinois and passed over Indiana, Ohio, and Pennsylvania. The bottom panel (b) shows results for West Virginia for an air mass that originated four days earlier in Missouri and crossed over the Ohio River Valley. Source: Sillman et al. 1990.

differences in vegetative cover (Matthews 1983). Average rates for emission of NO_x were estimated in the range $1.5 - 3.4 \times 10^{11}$ mol cm^{-2} sec^{-1}. Emissions of anthropogenic hydrocarbons over the region varied between 3.5×10^{11} and 1.5×10^{12} mol cm^{-2} sec^{-1}, as compared with emissions of isoprene in the range $7.5 - 19 \times 10^{11}$ mol cm^{-2} sec^{-1}.

Emissions in Figure 17.12 are expressed as multiples of emissions rates estimated by NAPAP. Note that, assuming scale factors of unity for both NO_x and anthropogenic hydrocarbons (the most likely range for the associated emissions), predicted levels of O_3 exceed, for both regions, standards mandated by the United States Environmental Protection Agency (EPA). The most recent regulations, issued in 1997,

define a maximum 8-hour permissible average concentration for O_3 of 80 ppb, mandating that this standard should not be exceeded on more than three occasions over the course of a year. From the pattern of the results displayed in Figure 17.12, it is clear that conditions for O_3 formation lie in the NO_x-limited regime. Reducing emissions of anthropogenic hydrocarbons would have little effect on O_3; the analysis suggests that if O_3 levels are to be reduced to acceptable levels during smog episodes during summer in the rural eastern United States, it will be necessary to implement steps to reduce emissions of NO_x.

Results for a region subject to the influence of air plumes originating from urban environments are summarized in Figure 17.13. Results are presented in this case as functions of scale factors referenced with respect to the magnitude of emissions of NO_x and anthropogenic hydrocarbons expected for urban regions. Predicted levels of O_3 are significantly higher than values indicated in Figure 17.12, in excess of 140 ppb, assuming the most likely levels of emissions (scale factors of one). Conditions for production of O_3 appear to lie close to the boundary between NO_x and hydrocarbon limitation. A reduction in O_3 would appear to dictate a strategy to reduce emissions of both NO_x and hydrocarbons. Paradoxically, as previously noted, it would be possible to achieve a reduction in O_3 in the vicinity of the urban plume by *increasing* emissions of NO_x. Benefits for the urban hinterland would be achieved, however, at the expense of the down-wind environment. Export of excess NO_x from urban regions would result in enhanced production of O_3 elsewhere.

In summary, it is clear that for most of the United States, while emissions of hydrocarbons are important for cities, the buildup of O_3 in the lower atmosphere during summer depends most critically on the supply of NO_x. Aggressive steps have been taken since the Clean Air Act was implemented in 1970 to regulate emissions of both NO_x and hydrocarbons. Emissions of industrial hydrocarbons in the United States declined by about 12 % between 1980 and 1995. It has proved more difficult, however, to reduce emissions of NO_x that remained relatively constant over this period. The transportation sector (cars and trucks) represents a dominant source of NO_x, especially in cities. An additional important contribution is associated with the generation of electric power by the combustion of fossil fuels. The number of vehicle miles driven per year increased by 60% over the past 15 years. It is clear, therefore, that the problem could have been much worse absent the steps taken to reduce emissions. Air quality in heavily polluted cities, such as Los Angeles, has improved significantly, most likely reflecting the reduction in emission of hydrocarbons, but continues to violate national standards. Full compliance with the Clean Air Act will require further, major reductions in emissions of NO_x. It is unlikely that these reductions can be achieved if we continue to rely on gas-guzzling cars for personal transportation. Hybrid vehicles, such as the Toyota Prius, or electrically powered vehicles, or modes of transportation based on new technologies such as the fuel cell, offer hope for the future. In the interim, we may hope for improvements in public transportation systems and for regional plans to reduce the hazards posed by uncontrolled urban sprawl.

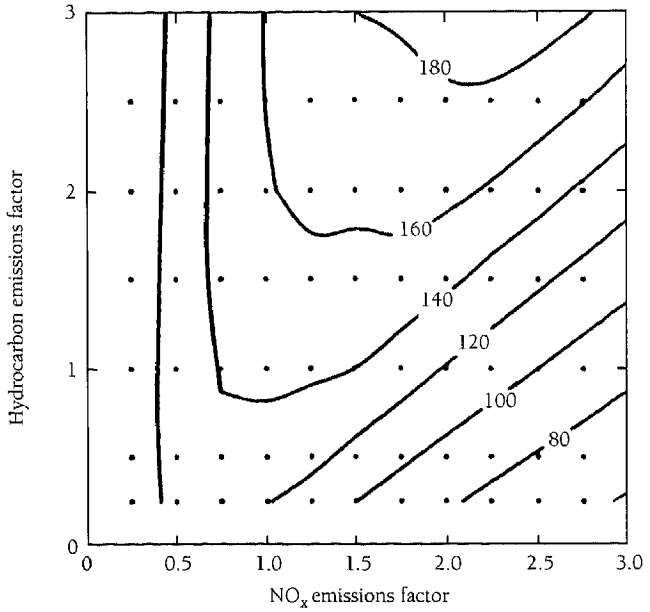

Figure 17.13 Peak ozone (in ppb) in the urban plume of New York, on the fourth day of ozone-episode simulations. Source: Sillman et al. 1990.

17.5 The Global Distribution of Tropospheric OH and the Oxidative Capacity of the Atmosphere

As noted at the outset, reactions with tropospheric OH play a critical role in removal from the atmosphere of a variety of gases ranging from CH_4 to CO, including the suite of industrially produced hydrocarbons discussed above. The abundance of tropospheric OH depends on the flux of ultraviolet solar radiation transmitted through the stratosphere to the lower atmosphere, on the intensity of radiation available to produce the $O(^1D)$ atom implicated in the primary source of OH (see reaction 17.6). It is sensitive, therefore, to the density of the overlying column density of O_3, to the abundance of O_3 present in the stratosphere. It is also sensitive to the abundances of O_3 and H_2O in the troposphere, the latter being, obviously, a function of temperature. We expect concentrations of OH in the troposphere to be highest at low latitudes and to vary significantly with the time of day. A realistic treatment of the role of tropospheric OH as a sink for specific atmospheric gases requires a comprehensive analysis of the factors responsible for its variation in space and time; in short, a global perspective.

Our discussion in this Section draws heavily on results of a recent study of the global, 3-dimensional distribution of tropospheric OH by Spivakovsky et al. (2000). In this study, distributions of O_3, CO, hydrocarbons, water vapor, oxides

of nitrogen, temperature, cloud cover, and column O_3 were specified, based on a composite of best available data. Concentrations of OH were calculated, solving the relevant chemical equations defining sources and sinks for OH and allowing appropriately for variations in the intensity of sunlight as a function of time of day. A summary of results, expressed in terms of zonal (longitudinal) averages, is presented for the months of January, April, July, and October in Table 17.3a–d. A graphical representation of these data is displayed in Plate 6 (top) (see color insert). Averaged over space and time, the analysis of Spivakovsky et al. (2000) implies a global average value for the concentration of OH in the troposphere of 1.16×10^6 mol cm^{-3}.

The sensitivity of OH to a number of key variables, notably the concentrations of tropospheric H_2O, O_3, NO_x, CO, and CH_4, and to the abundance of O_3 in the overlying stratospheric column, is summarized in Table 17.4. As expected, an increase (or decrease) in the abundance of either H_2O or O_3 should result in an increase (or decrease) in OH. The change in this case reflects the impact of the postulated change on the rate for production of OH by reaction (17.6). As indicated, an increase of 25% in both H_2O and O_3 should lead to a comparable, though slightly smaller (20%), increase in OH, with the sensitivity to H_2O somewhat greater than that for O_3. An increase (or decrease) in NO_x should result in a modest change of the same sign in OH, reflecting the impact of the change in NO_x on the rate for recycling of HO_x by (17.16). An increase (or decrease) in CO or CH_4 should lead to a small change of the opposite sign in OH, corresponding to the change in the loss frequency for OH (rates for reactions 17.12 and 17.13). Results are most sensitive to an adjustment in the overlying column of O_3. As indicated, a decrease of 25% in column O_3, leading to an increase in transmission of ultraviolet solar radiation, would result in an increase of similar magnitude (26%) in OH. Note that the response of OH to column O_3 is asymmetric: greater when the column density is reduced, reflecting the exponential dependence of the transmission of solar radiation on the column density of O_3.

Observations of methyl chloroform (CH_3CCl_3) provide an important check on the accuracy of the computed distribution of OH. Methyl chloroform is an industrial solvent: chemical industry accounts for the only known source of the gas in the atmosphere. It is removed mainly by reaction with tropospheric OH, with additional loss due to stratospheric oxidation (by photolysis and reaction with OH) and, at a significantly smaller rate, due to uptake by the ocean. It is thought that the source is known to an accuracy of about ±5%. Model results are compared with observations from a number of locations around the world (Prinn et al. 1995) in Figure 17.14. The Figure includes results from model simulations where concentrations of OH were allowed to vary over a range of ±25% (dotted lines). The

Table 17.3a Zonally and Monthly Averaged OH Concentrations for January (10^5 mol cm^{-3}).

	1000 hPa	*900 hPa*	*800 hPa*	*700 hPa*	*500 hPa*	*300 hPa*	*200 hPa*
90°N	--	--	--	--	--	--	--
84°N	--	--	--	--	--	--	--
76°N	--	--	--	--	--	--	--
68°N	0.0	0.0	0.0	0.0	0.0	0.0	0.0
60°N	0.2	0.2	0.2	0.2	0.2	0.2	0.2
52°N	0.4	0.4	0.8	0.6	0.6	0.7	0.8
44°N	0.7	0.9	1.8	1.4	1.6	1.6	1.7
36°N	1.7	2.1	3.6	3.3	3.7	3.5	3.5
28°N	4.3	5.1	6.2	7.1	6.4	4.5	4.6
20°N	7.3	9.2	11.4	12.2	10.0	6.4	5.9
12°N	10.0	13.7	16.3	16.0	14.3	8.5	7.2
4°N	7.0	11.2	15.4	18.5	20.7	11.2	9.2
4°N	7.1	10.9	15.5	20.2	23.0	12.8	9.6
12°N	8.9	13.1	18.4	22.8	26.1	14.2	11.1
20°N	10.2	16.0	24.5	26.6	25.6	14.6	11.2
28°N	10.5	15.8	24.4	26.1	24.3	14.8	11.4
36°N	9.6	13.8	18.4	21.1	21.1	14.7	11.8
44°N	6.2	8.1	11.0	16.2	18.9	14.2	11.4
52°N	4.1	5.1	7.4	12.5	15.5	12.7	10.2
60°N	3.0	3.7	5.2	9.9	12.0	11.0	9.3
68°N	4.5	7.2	7.3	8.6	8.9	9.6	9.0
76°N	4.0	5.0	5.0	6.8	7.3	8.5	8.9
84°N	4.7	5.0	5.0	6.4	6.6	7.9	8.9
90°N	--	--	--	6.5	6.6	7.7	8.6

From Spivakovsky et al. (2000).

Table 17.3b Zonally and Monthly Averaged OH Concentrations for April (10^5mol cm^{-3}).

	1000 hPa	900 hPa	800 hPa	700 hPa	500 hPa	300 hPa	200 hPa
90°N	0.4	0.6	0.8	1.0	0.8	0.9	1.3
84°N	0.3	0.5	0.6	0.8	1.0	1.1	1.5
76°N	0.5	0.7	0.9	1.4	1.4	1.6	2.1
68°N	3.9	3.5	3.4	3.2	2.2	2.3	2.7
60°N	3.8	4.1	5.0	4.4	3.5	3.2	3.3
52°N	4.9	5.3	7.1	6.0	5.1	4.2	4.0
44°N	7.8	8.7	11.0	8.8	7.7	5.6	5.0
36°N	9.0	11.9	13.8	12.7	11.3	7.5	6.4
28°N	12.4	14.8	17.1	18.1	14.8	7.9	6.9
20°N	15.1	18.9	21.4	23.7	17.8	9.6	8.0
12°N	14.3	19.4	22.1	23.5	20.4	10.4	8.4
4°N	7.7	14.1	18.8	22.4	23.5	12.3	10.0
4°N	7.1	13.4	16.0	20.8	22.3	12.7	10.6
12°N	7.3	13.6	15.9	19.1	19.8	12.0	10.7
20°N	8.7	12.8	16.8	18.4	16.7	11.0	9.6
28°N	7.9	10.4	12.9	14.1	13.6	9.7	8.6
36°N	5.8	6.8	8.0	9.6	10.5	8.0	6.9
44°N	2.7	3.1	3.9	5.5	7.5	6.1	5.6
52°N	1.1	1.4	1.7	2.8	4.3	4.0	3.4
60°N	0.4	0.5	0.7	1.3	2.1	2.1	1.8
68°N	0.2	0.3	0.3	0.5	0.7	0.8	0.7
76°N	0.1	0.1	0.1	0.1	0.2	0.1	0.2
84°N	0.0	0.0	0.0	0.1	0.1	0.0	0.0
90°N	--	--	--	--	--	--	--

From Spivakovsky et al. (2000).

model allowed for loss of CH_3CCl_3 in the stratosphere but did not account for removal by the ocean. With the standard OH model (solid line in Figure 17.14), 11% of the global loss of CH_3CCl_3 occurs in the stratosphere with the balance (89%) in the troposphere. Agreement between model and observation is excellent using the computed distribution of OH; it could be improved somewhat if OH concentrations were reduced by about 3% and if we allowed for a small sink due to the ocean. Based on a consideration of all of the available sources of information, Spivakovsky believes that the distributions of OH summarized in Table 17.3 and Plate 6 (top) should be accurate to within about ±10%.

The change with time of the abundance of a gas X, which is well-mixed throughout the atmosphere but removed mainly by reaction with OH in the troposphere, may be expressed in terms of an equation of the form

$$\frac{dN}{dt} = P(t) - (0.85)\, N(t)\, \nu, \qquad (17.84)$$

where $N(t)$ defines the total number of X molecules present in the atmosphere at time t, $P(t)$ denotes the magnitude of the source (mol sec^{-1}) and ν is a frequency (sec^{-1}) associated with the loss of X by reaction with tropospheric OH. The factor of 0.85 accounts for the fact that the loss process is assumed to be confined to the troposphere, and only 85% of the total mass of X in the atmosphere resides in the troposphere.[9] In steady state ($dN/dt = 0$), it follows that

$$N(t) = P(t)\left[(0.85)\,\nu\right]^{-1} = P(t)\,\tau, \qquad (17.85)$$

where

$$\tau = \left[(0.85)\,\nu\right]^{-1} \qquad (17.86)$$

may be identified with the lifetime of X with respect to removal by tropospheric OH. Note that τ defines the time required for production to supply a quantity of X sufficient to fill the atmospheric reservoir to content N, starting from zero, if loss were eliminated. Equivalently, if the source were eliminated, τ would define the time required for the concentration of X to decline by a factor of e.[9]

Spivakovsky et al. (2000) showed that the lifetime of a long-lived gas X toward removal by reaction with tropospheric OH may be estimated with adequate precision using the relation

$$\tau_X = (0.85\ [\mathrm{OH}]\ k_X\ )^{-1}, \qquad (17.87)$$

where [OH] defines an average value for the concentration of OH in the troposphere and k_X denotes an appropriate average value for the rate constant for reaction of OH with X. They showed that little error is introduced by using the spatially and temporally averaged value for the concentration of OH (1.16×10^6 cm^{-3}, as noted above), assuming a value for k_X appropriate for a temperature of 270K. With these assumptions, as indicated by the following Example, the lifetime of CH_3CCl_3 toward removal by OH in the troposphere is estimated at 5.7 yr. The lifetime reflecting removal by the stratosphere and ocean in addition to the troposphere is estimated (Example 17.22) at 4.6 yr. This compares favorably

Table 17.3c Zonally and Monthly Averaged Concentrations of OH for July (10^5mol cm^{-3}).

	1000 hPa	900 hPa	800 hPa	700 hPa	500 hPa	300 hPa	200 hPa
90°N	5.5	7.4	8.3	10.0	9.7	6.9	8.8
84°N	3.8	5.2	6.4	8.6	10.9	7.7	9.5
76°N	3.7	5.1	6.9	9.7	11.5	7.6	8.4
68°N	7.4	11.6	13.9	15.4	13.2	8.2	7.7
60°N	6.2	10.6	16.2	17.0	15.3	9.2	8.0
52°N	6.2	11.8	19.5	19.4	17.5	10.6	8.6
44°N	12.3	23.1	26.9	25.1	22.1	12.6	10.0
36°N	14.9	24.7	27.9	28.0	25.0	14.4	11.3
28°N	12.6	17.9	22.7	24.7	23.3	12.3	8.8
20°N	13.0	17.6	21.9	26.5	24.8	13.7	10.0
12°N	10.9	16.4	20.1	24.4	24.8	13.6	10.0
4°N	10.3	14.6	19.2	22.3	23.2	12.9	10.2
4°N	10.4	15.4	20.4	21.3	20.1	12.4	10.9
12°N	9.9	13.8	17.0	17.8	15.9	10.5	9.9
20°N	7.9	10.9	12.7	13.1	11.3	8.6	7.8
28°N	4.5	5.6	6.2	7.1	7.1	5.8	5.8
36°N	2.6	2.8	3.2	4.0	4.6	3.7	3.3
44°N	0.9	1.0	1.2	1.9	2.6	2.2	1.9
52°N	0.3	0.3	0.4	0.7	1.1	1.0	0.9
60°N	0.1	0.1	0.1	0.2	0.3	0.2	0.2
68°N	0.0	0.0	0.0	0.0	0.0	0.0	0.0
76°N	--	--	--	--	--	--	--
84°N	--	--	--	--	--	--	--
90°N	--	--	--	--	--	--	--

From Spivakovsky et al. (2000).

with the lifetime of 4.8 yr. inferred from a purely empirical analysis of the observational data (Prinn et al. 1995).

Example 17.21: The rate constant for reaction of OH with CH_3CCl_3 has a value of 5.62×10^{-15} cm^{-3} sec^{-1} for a temperature characteristic of the mid troposphere. Assuming an average concentration of tropospheric OH equal to 1.16×10^6 cm^{-3}, estimate the lifetime of CH_3CCl_3 as determined by reaction with tropospheric OH.

Answer: The lifetime is given by equation (17.86). Substituting for [OH] and k_x, we find

$$\begin{aligned}\tau_{CH_3CCl_3} &= \left[(0.85)(1.16 \times 10^6)(5.62 \times 10^{-15})\right]^{-1} \text{ sec} \\ &= (5.54 \times 10^{-9})^{-1} \text{ sec} \\ &= 1.8 \times 10^8 \text{ sec} \\ &= 5.7 \text{ years}\end{aligned}$$

■

Example 17.22: Methyl chloroform is also removed in the stratosphere with an effective lifetime estimated at 34 yr. It is removed also by the ocean, with a lifetime estimated at 80 yr. Use the results in Example 17.21 to calculate the composite lifetime for CH_3CCl_3, reflecting removal by the combination of troposphere, stratosphere, and ocean.

Answer: To estimate the composite lifetime, we must combine first the loss frequencies associated with the separate processes. To find the composite lifetime, we must estimate first the net rate for removal. (Note that the composite lifetime *cannot* be derived by adding lifetimes for component loss processes.)

$$\begin{aligned}\tau_{CH_3CCl_3} &= \left[(\tau_{trop})^{-1} + (\tau_{strat})^{-1} + (\tau_{ocean})^{-1}\right]^{-1} \text{ yr} \\ &= \left[(5.7)^{-1} + (34)^{-1} + (80)^{-1}\right]^{-1} \text{ yr} \\ &= [0.175 + 0.029 + 0.013]^{-1} \text{ yr} \\ &= (0.217)^{-1} \text{ yr} \\ &= 4.6 \text{ years}\end{aligned}$$

■

Lifetimes set by reaction with tropospheric OH are presented for a number of industrial hydrofluorocarbons (HFCs) and hydrochlorofluorocarbons (HFCs) in Table 17.5. The Table also includes results for CH_4, CH_3Cl, CH_3Br, CH_2CCl_2, and C_2Cl_4. Lifetimes summarized here were calculated in the same manner as for CH_3CCl_3 (also included in the Table).

17.6 The Budget of Tropospheric Ozone

As noted earlier, O_3 enters the troposphere in part by transport downward from the stratosphere, in part by production in situ through reactions (17.72)–(17.75). It is removed in

Table 17.3d Zonally and Monthly Averaged Concentrations of OH for December (10^5mol cm^{-3}).

	1000 hPa	900 hPa	800 hPa	700 hPa	500 hPa	300 hPa	200 hPa
90°N	--	--	--	--	--	--	--
84°N	0.0	0.0	0.0	0.0	0.0	0.0	0.0
76°N	0.1	0.1	0.1	0.1	0.1	0.1	0.1
68°N	0.5	0.5	0.5	0.6	0.5	0.4	0.6
60°N	0.8	0.9	1.2	1.2	1.5	1.3	1.5
52°N	1.7	1.9	2.9	2.6	3.1	2.8	2.9
44°N	4.4	4.7	6.5	5.3	5.7	4.9	5.1
36°N	6.3	8.3	10.1	9.2	9.0	7.3	7.5
28°N	9.4	12.0	13.5	13.2	11.3	7.0	6.5
20°N	10.1	13.9	15.3	16.0	14.6	8.8	8.0
12°N	9.9	15.3	17.4	19.1	20.1	10.6	8.8
4°N	8.4	13.5	19.1	23.7	25.1	12.4	9.9
4°N	11.4	18.5	24.5	28.8	28.0	14.3	11.2
12°N	13.7	19.5	25.5	29.6	26.7	13.9	11.1
20°N	13.1	19.5	23.8	27.1	22.2	13.6	10.4
28°N	9.2	13.0	16.0	19.3	17.2	10.6	9.1
36°N	8.0	9.4	11.0	13.5	13.4	8.9	7.4
44°N	4.9	5.6	7.0	10.2	10.6	7.2	6.1
52°N	3.0	3.5	4.5	6.9	7.5	6.0	5.3
60°N	2.7	2.9	3.2	4.5	5.4	5.6	5.1
68°N	2.7	3.4	3.3	3.7	3.6	5.3	5.2
76°N	1.2	1.6	1.0	1.7	1.9	3.4	3.4
84°N	0.0	0.9	0.9	1.0	1.3	2.3	2.2
90°N	--	--	--	0.8	1.1	1.7	1.6

From Spivakovsky et al. (2000).

Table 17.4 Relative Change (%) in the Global-Mean OH Concentration.

Scaling of Precursors	−50%	−25%	25%	50%
H_2O	−24	−11	10	20
O_3	−15	−8	8	17
O_3 and H_2O	−31	−18	20	43
NO_x	−17	−8	8	14
CO	23	10	−8	−14
CH_4	14	6	−5	−10
O_3 column	71	26	−17	−28

From Spivakovsky et al. 2000. Concentrations are in response to a uniform scaling of concentrations of precursors globally by ±25% and ±50%.

the gas phase by (17.6), (17.17), (17.21), and (17.31), with additional loss due to contact with organic matter at the surface (dry deposition).

Production of O_3 requires a supply of reduced species–hydrocarbons and CO–and, most critically, a source of NO_x. It is also sensitive to the flux of ultraviolet solar radiation reaching the troposphere. The lifetime of O_3 in the troposphere ranges from months at high latitudes during winter, decreasing to weeks at high latitude during summer, and declining to days in the tropics. Lifetimes are shortest at low altitude, increasing to hundreds of days in the upper troposphere. The source of O_3 is largest over continents and over industrial regions during summer. Significant production takes place in the tropics, especially in regions subject to seasonal emissions of NO_x and hydrocarbons associated with the burning of biomass. It comes as no great surprise that the abundance of O_3 is variable in space and time; a realistic treatment requires a 3-dimensional perspective. To be useful, a model for tropospheric O_3 must account for spatial and temporal variations in transport, for variations in emissions of hydrocarbons and NO_x, and for changes in the overlying abundance of O_3 in the stratosphere. The analysis presented here is based on results of a 3-dimensional study reported by Wang et al. (1998a–c).

Wang et al. (1998a–c) accounted for both industrial and natural sources of CO, hydrocarbons, and NO_x; they allowed in addition for the influence of biomass burning. A summary of assumptions of their model with respect to sources for NO_x, CO, and various hydrocarbons is given in Table 17.6. Spatial distributions of O_3 calculated for the surface and for the level in the atmosphere corresponding to a pressure of 500 mb are presented for the months of January and July in Plate 6 (bottom) (see color insert). Note the preponderance of elevated levels of O_3 over industrial regions of the Northern

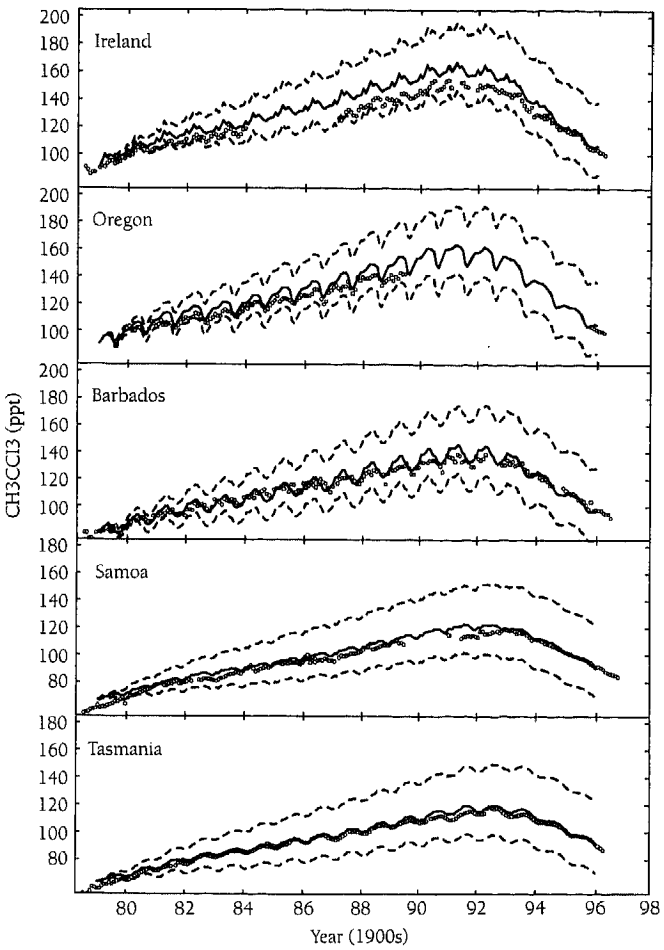

Figure 17.14 Observed long-term trend in CH_3CCl_3 (dots) simulated using standard OH without the ocean sink (solid lines), and with tropospheric loss frequencies reduced and increased by 25% (dashed lines). Source: Prinn et al. 1995.

Hemisphere during summer and over regions of the tropics subject to seasonal inputs due to burning of biomass during the dry season. Zonally averaged values for the chemical lifetime of O_3 as a function of latitude and altitude are given in Figure 17.15. Composite budgets (spatially integrated sources and sinks) for O_3 for the Northern and Southern Hemispheres and for the globe are summarized in Table 17.7.

The results in Table 17.7 suggest that the rate at which O_3 is produced by tropospheric chemical reactions exceeds the rate at which it is supplied by transport from the stratosphere on a global scale by more than a factor of ten. The source of O_3 in the Northern Hemisphere is larger than that in the Southern Hemisphere by more than 70%, reflecting primarily the importance of the higher (a factor of 3.5) source of NO_x in the north. The abundance of O_3 in the Northern Hemisphere is larger than that in the Southern Hemisphere by about 40%. The lifetime of O_3, averaged over the entire global troposphere, is estimated as 25 days, slightly longer for the Southern as compared to the Northern Hemisphere: 28 days as compared to 23 days.

The data in Table 17.6 indicate emissions of NO_x in the Northern Hemisphere of 3.3×10^{13} g N yr^{-1}, resulting

Table 17.5 Lifetimes for Gases Removed by Reaction with Tropospheric OH.

Species	*Common Name*	*Lifetime (yrs)*
CH_3F	HFC-41	2.8
CH_2F_2	HFC-32	5.3
CHF_3	HFC-23	25.1
CH_2FCl	HCFC-31	1.3
$CHFCl_2$	HCFC-21	2.0
CHF_2Cl	HCFC-22	12.0
CH_3CH_2F	HFC-161	0.3
CH_2FCH_2F	HFC-152	0.5
CH_3CHF_2	HFC-152a	1.5
CH_2FCHF_2	HFC-143	3.6
CH_3CF_3	HFC-143a	53.0
CHF_2CHF_2	HFC-134	10.0
CH_2FCF_3	HFC-134a	13.8
CHF_2CF_3	HFC-125	30.9
CH_3CFCl_2	HCFC-141b	10.2
CH_3CF_2Cl	HCFC-142b	19.1
CH_2ClCF_2Cl	HCFC-132b	3.3
CH_2ClCF_3	HCFC-133a	3.7
$CHCl_2CF_3$	HCFC-123	1.3
$CHFClCF_3$	HCFC-124	6.0
CH_4	--	9.2
CH_3Cl	--	1.4
CH_3Br	--	1.9
CH_3CCl_3	--	5.6
CH_2Cl_2	--	0.4
C_2Cl_4	--	0.3

in an in situ source of O_3 of 2.62×10^{15} g O_3 yr^{-1} (Table 17.7). This implies a yield for O_3 per molecule of NO_x of 23 molecules per molecule (the factor 14/48 accounts for the difference in masses of O_3 and N): the corresponding yield for the Southern Hemisphere is 46 molecules per molecule. The yield of O_3 per NO_x molecule depends on the relative rates for reactions (17.21) and (17.16), allowing for additional production by (17.72). If we assume that production of O_3 is balanced primarily by in situ chemical loss and that loss proceeds primarily by (17.6), it follows that production of a molecule of O_3 should be associated with production of approximately three molecules of OH.[10] If oxidation of reduced species provides the dominant sink for OH (reactions of the form 17.70), it follows that the integrated rate for production of O_3 should be equal to approximately one-third of the rate at which reduced species are consumed in the troposphere. Assuming that (17.21) provides the dominant sink for NO_x, it follows that the yield for O_3 per molecule of NO_x, ϵ, should be given by

$$\epsilon = \frac{\text{production of } O_3}{\text{loss of } NO_x} = \frac{S_c}{3S_n}, \qquad (17.88)$$

where S_c indicates the magnitude of the source for reduced species and S_n defines the corresponding magnitude of the

*Table 17.6 Sources of NO_x, CO, Ethane, Propane, $\geq C_4$ Alkanes, $\geq C_3$ Alkenes, Isoprene, and Acetone.**

	Global	*Northern Hemisphere*	*Southern Hemisphere*
NO_x			
Fossil fuel combustion	21	20	1.2
Biomass burning	11.6	6.5	5.1
Soil	6.0	4.2	1.8
Lightning	3.0	1.7	1.3
Aircraft	0.51	0.47	0.04
Stratosphere[a]	0.10	0.006	0.04
Total	42	33	9.4
CO			
Fossil and wood fuel combustion, industry	520	480	40
Biomass burning	520	290	230
CH_4 oxidation[b]	800	460	340
NMHC oxidation[b]	290	170	120
Total	2130	1400	730
Ethane			
Industry	6.3	5.7	0.6
Biomass burning	2.5	1.4	1.1
Total	8.8	7.1	1.7
Propane[c]			
Industry	6.8	6.1	0.7
Biomass burning	1.0	0.92	0.08
Total	7.8	7.0	0.8
$\geq C_4$ alkanes			
Industry	30	27	3
$\geq C_3$ alkenes			
Industry	10.4	9	1.4
Biomass burning[d]	12.6	7	5.6
Total	23	16	7
Isoprene			
Vegetation	597	297	300
Acetone			
Industry	1.0	0.9	0.1
Biomass burning	8.9	5.0	3.9
Vegetation	15	7.5	7.5
Oxidation of propane	6.2	5.3	0.9
Oxidation of higher alkanes[b]	6.2	5.5	0.7
Total	37	24	13

**-As assumed in the 3-dimensional simulation of the chemistry of the troposphere described by Wang et al. 1998a.*

Units are Tg (10^{12} g) N yr^{-1} for NO_x, Tg CO yr^{-1} for CO, and Tg C yr^{-1} for NMHCs.

[a]Downward transport of NO_x across the tropopause. This transport also supplies 0.38 Tg N yr^{-1} of HNO_3 globally.

[b]Computed within the model.

[c]Included in the model as a direct emission of acetone; the yield of acetone from oxidation of propane is specified as 80% (Singh et al. 1994).

[d]Including 6 Tg C yr^{-1} of $\geq C_2$ aldehydes.

source for NO_x.[11] The lower value of the yield for O_3 inferred for the Northern Hemisphere may be attributed to the higher value for the associated source of NO_x.

Equation (17.88) implies that, integrated over a large region (a hemisphere, for example), the source of O_3 (obtained by multiplying the yield per NO_x molecule by the total source of NO_x) should be proportional to S_c: the input of reduced species (hydrocarbons and CO). This analysis suggests that production of O_3 should be independent of S_n, the source of NO_x. It follows with our assumptions, since removal of O_3 is proportional to the abundance of O_3, that the integrated abundance of O_3 should also be proportional to S_c and independent of S_n. This apparently contradicts the result obtained earlier: that production of O_3 in the NO_x-

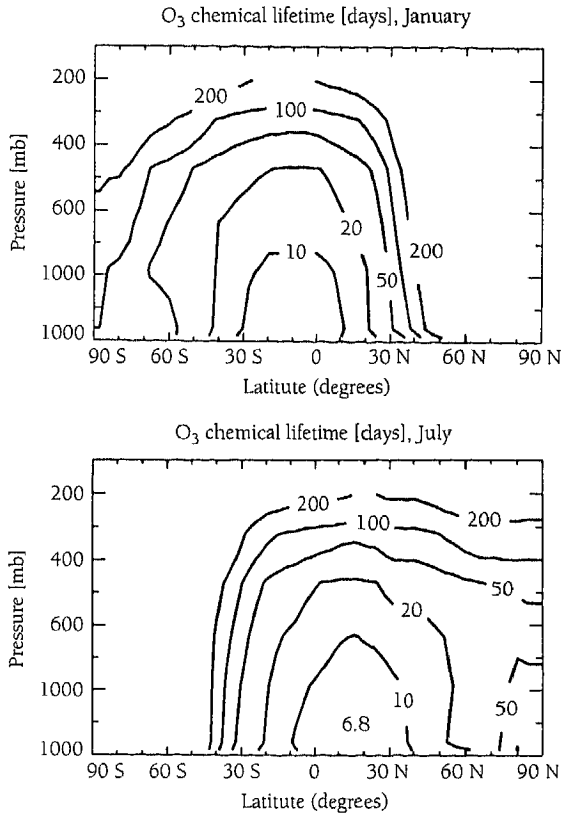

Figure 17.15 Lifetimes (days) for O_3 as a function of pressure (altitude) and latitude, calculated using model values for O_3 concentrations together with model estimates for rates of chemical removal. Source: Wang et al. 1995.

limited regime should be proportional to the abundance of NO_x but independent of the abundance of hydrocarbons. The contradiction arises from our neglect of such loss processes for O_3 as dry deposition, reactions (17.17) and (17.54), which together amount to about one-third of total loss of O_3. In fact, $S_c/3$ provides a lower limit for production of O_3, assuming that the flux of O_3 from the straosphere is small (Wang and Jacob 1998). It follows that strategies designed to address problems of elevated O_3, in not only urban but also remote regions, must provide for reduction of emissions of *all* relevant sources of pollution—hydrocarbons, CO, and NO_x.

While the most serious effects of anthropogenic emissions of hydrocarbons and NO_x on O_3 are as yet confined largely to industrial regions of the Northern Hemisphere and to selected regions of the tropics, there are troubling indications that the impact may be spreading. Wang, Logan, and Jacob (1998b) concluded that Asian pollution is already responsible for a detectable rise in the level and seasonal dependence of O_3 observed at the remote, high-altitude Mauna Loa Observatory in Hawaii. They attribute this effect to long-range transport of O_3 from Asia, noting that the lifetime of O_3 at the altitude of the Observatory (with a pressure level of 650 mb) is about 20 days.

The lifetime of NO_x is relatively brief, about a day. The impact of anthropogenic sources of NO_x may be extended, however, to larger spatial scales, if the compound is converted to longer-lived forms such as peroxyacetylnitrate (PAN, $CH_3C(O)OONO_2$, where (O) indicates that the O atom is double-bonded to the neighboring C atom). PAN is produced by photochemical oxidation of carbonyl species in

*Table 17.7 Contributions to the Budget of Tropospheric Ozone for the Northern Hemisphere, Southern Hemisphere, and Globe.**

	Global	*Northern Hemisphere*	*Southern Hemisphere*
Sources, Tg O_3 yr^{-1}			
In situ chemical production[a]	4100	2620	1480
Transport from stratosphere	400	240	160
Total	4500	2860	1640
Sinks, Tg O_3 yr^{-1}			
In situ chemical loss[b]	3680	2290	1390
Dry deposition	820	530	290
Total	4500	2820	1680
Interhemispheric transport, Tg O_3 yr^{-1}	0	–40	40
Burden, Tg O_3	310	180	130
Residence time, days	25	23	28

**-Due to: (1) in situ chemical production; (2) transport from the stratosphere; (3) in situ chemical loss; (4) loss at the surface, and (5) exchange between the hemispheres. The budget is for the air column extending up to 150 mbar. Annual mean budget terms are given for the odd oxygen family ($O_x = O_3 + O + NO_2 + HNO_4 + 2 \times NO_3 + 3 \times N_2O_5 + PANs + HNO_3$) to account for chemical interconversion between ozone and other components of O_x. Since ozone accounts for over 95% of O_x, the budgets of ozone and O_x can be regarded as equivalent. From Wang et al. 1998b.*

[a]Mainly from the reactions of peroxy radicals with NO.

[b]Mainly from the reactions $O^1D + H_2O$, $O_3 + HO_2$, and $O_3 + OH$.

the presence of NO_x. The key steps in formation of PAN from acetaldehyde (CH_3CHO) may be summarized as follows (Seinfeld and Pandis 1998):

$$CH_3CHO + OH \rightarrow CH_3CO + H_2O \quad (17.89)$$

$$CH_3CO + O_2 \rightarrow CH_3C(O)O_2 \quad (17.90)$$

$$CH_3C(O)O_2 + NO_2 + M \rightarrow CH_3C(O)O_2NO_2 + M \quad (17.91)$$

$$CH_3C(O)O_2NO_2 + M \rightarrow CH_3C(O)O_2 + NO_2 + M \quad (17.92)$$

The lifetime of PAN, determined by reaction (17.92), is a sensitive function of temperature, ranging from hours in warmer regions of the lower atmosphere, to months at colder temperatures characteristic of mid levels of the troposphere. The concern is that PAN, formed in polluted regions of the atmosphere where the abundance of NO_x is high, may be mixed upward into colder regions of the middle troposphere where the compound is comparatively stable. As PAN, NO_x may be transported over large spatial scales. Returning to lower, warmer regions of the atmosphere, it will decompose (by reaction 17.92), providing a distributed source of NO_x, thus extending the influence of local sources of NO_x pollution potentially to global scale.

The Harvard 3-dimensional model has been applied also in an attempt to simulate the abundance of O_3 in the preindustrial troposphere. Wang and Jacob (1998) concluded that the global abundance of O_3 was about 38% lower in the preindustrial environment as compared to today, 4.0×10^{12} moles as compared to 6.5×10^{12} moles. Similar to today, they found that the rate for in situ production of O_3 in the preindustrial troposphere was larger than the rate at which O_3 was supplied from the stratosphere. Similar again to today, they concluded that production of O_3 in the preindustrial environment was limited by NO_x. Globally averaged, they inferred a yield for O_3 of 58 molecules O_3 per molecule NO_x, higher than the contemporary value by about a factor of two, consistent with (17.88), given that the decrease in S_n for the preindustrial environment was larger than that for S_c (by a factor of 4.7, as compared to a factor of 2.6). They concluded that the globally averaged value for the concentration of OH in the preindustrial troposphere was about the same as today, consistent with the expectation that the concentration of OH should vary approximately as $S_n/S_c^{3/2}$, as implied by the analysis in Example 17.23.

Example 17.23: Estimate how the abundances of HO_2 and OH would be expected to vary as functions of S_c and S_n. Assume that production of O_3 is NO_x limited and that HO_2 is removed primarily by reaction with NO rather than O_3. Assume further that the relative abundances of NO and NO_2 are determined by reactions (17.39) and (17.40) and that production of O_3 and the abundance of O_3 are proportional to S_c, as indicated above.

Answer: With our assumptions, $[HO_2]$ is given by (17.35). Hence,

$$[HO_2] \approx [O_3]^{1/2} \approx S_c^{1/2}$$

Loss of NO_x proceeds primarily by (17.21). Thus,

$$[OH] \approx S_n / [NO_2]$$

Since the relative abundances of NO and NO_2 are determined by (17.39) and (17.40), it follows that

$$[NO_2] \approx [NO][O_3]$$

But production of O_3, P_{O_3}, is determined by the rate for reaction (17.16). Thus

$$P_{O_3} \approx [NO][HO_2] \approx [NO]\, S_c^{1/2}$$

Using (17.88), it follows that

$$[NO] \approx P_{O_3} / S_c^{1/2} \approx S_c^{1/2},$$

and hence,

$$[NO_2] \approx S_c^{1/2}\,[O_3] \approx S_c^{3/2}$$

Thus,

$$[OH] \approx \frac{S_n}{[NO_2]} \approx \frac{S_n}{S_c^{3/2}} \quad \blacksquare$$

Wang and Jacob (1998) assumed an abundance of CH_4 for the preindustrial environment of 0.7 ppm, as inferred from studies of gases trapped in polar ice (see Figure 5.5). Given that the abundance of OH for the preindustrial environment is expected to be approximately the same as today, it follows that the increase in the abundance of CH_4 in the atmosphere over the past several hundred years should be attributed primarily to an increase in the magnitude of the source. The increase in concentration from 0.7 ppm to about 1.7 ppm implies an increase in emissions by about a factor of 2.4. We return to this matter below in the context of our discussion of the CH_4 budget.

17.7 The Budget of Atmospheric Methane

As illustrated in Figure 5.5, the mixing ratio of CH_4 was relatively constant, at a little less than 700 ppb, from around A.D. 1000 to about the midpoint of the eighteenth century. It has more than doubled, rising from 650 ppb to close to 1700 ppb over the past 250 years. Accepting the conclusion of Wang and Jacob (1998) that the abundance of OH in the preindustrial environment was similar to today, it follows that production of CH_4 increased by about a factor of 2.4 over the past 250 years, from about 230 Tg yr^{-1} in 1750 (1 Tg = 10^{12} g) to more than 550 Tg yr^{-1} today. The long-term trend in the source, assuming constant OH, is illustrated in Figure 17.16.[12] The growth rate was particularly rapid after World War II, reaching a maximum in the early 1980s (Etheridge et al. 1998) as indicated in Figure 17.17. Observations for the most recent period suggest that production has been relatively constant since about 1984 (Dlugokencky et al. 1998).

Estimates of contributions from individual sources and sinks, reported by a number of authors over the past several years, are presented in Table 17.8. It seems reasonable to assume that production prior to A.D. 1750 was dominated by wetlands (with minor contributions from biomass burning,

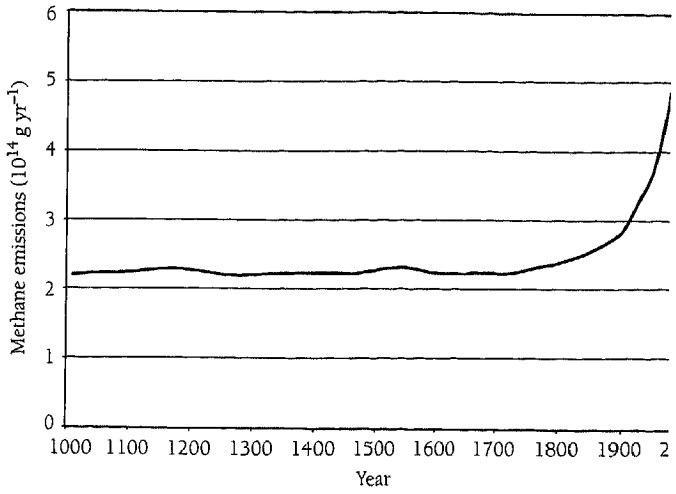

Figure 17.16 The long term trend in emissions of CH_4, assuming constant OH.

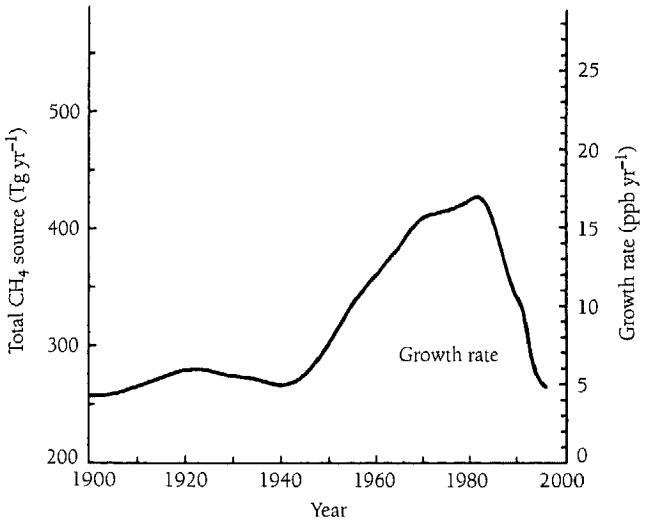

Figure 17.17 The growth rate of CH_4 emissions over time.

Table 17.8 CH_4 Budget (Tg yr^{-1})

	WMO (1995)	*Fung et al. (1991)*	*Hein, Crutzen, and Heimann (1997)*
Wetlands	110	115	232
Termites	20	20	--
Ocean + Freshwater	15	10	--
Hydrates	10	5	--
Energy-related	100	75	103
Sewage Treatment	25	--	--
Landfills	30	40	40
Animal Waste	25	--	--
Ruminants	80	80	90
Biomass Burning	40	55	41
Rice Paddies	60	100	69
Total Sources	515	500	575
Soils	30	10	28
Reaction with OH	445	450	469
Removal in stratosphere	40	--	44
Total sinks	515	460	541

termites, and ruminants) and to adopt an estimate for the source strength of about 230 Tg yr^{-1}, as indicated by the argument presented above. We note that this value is consistent with the result for wetlands quoted by Hein, Crutzen, and Heimann (1997). The growth in emission of CH_4 over the past several hundred years must be attributed, it appears, to human activity. The important influences include: agricultural practices favoring cultivation of rice; an expanding population of domestic ruminants, mainly cattle, sheep, and goats; burning of vegetation to clear land, largely in the tropics and primarily for purposes of agriculture; increased use of fossil fuels; and disposal of concentrated organic waste produced by an increasingly urbanized society.

The bulk of the sources indicated in Table 17.8 reflect production by bacteria from the biological kingdom known as the *Archaebacteria*. Commonly referred to as *methanogens*, these organisms are obligatory anaerobes; that is to say, they are capable of growth only under conditions where the abundance of oxygen is extremely low. They proliferate in organic-rich sediments as found, for example, in natural swamps or in flooded, rich paddy fields, where the supply of oxygen to sediments is limited by high rates for biological consumption of oxygen in the overlying water column. They play an important role also in the digestive tracts of grass-feeding (herbivorous) animals, such as cattle, sheep, goats, camels, buffalo, and deer. Plant material eaten by these animals is temporarily stored in the rumen (the first compartment of the stomach, hence the collective reference to these species as *ruminants*), where it is transformed to more digestible organic matter by a complex population of anaerobic bacteria. The relationship between ruminants and methanogenic bacteria is symbiotic: ruminants feed the bacteria; in turn, the bacteria feed the ruminants. In the process, copious quantities of CH_4 are evolved and released to the atmosphere through a combination of belching and flatulence. A typical domestic cow produces as much as 200 liters of CH_4 per day (Wolin 1979). Given that there are more than a billion cattle in the world today (more than 100 million in

the United States alone), it is not surprising that cattle are thought to provide a significant, contemporary source of CH_4.

Trends in cattle population as a function of time are illustrated in Figure 17.18. The Figure also includes data on the area of land devoted to rice. It is interesting to note the rapid increase in both cattle population and rice acreage that took place after World War II. The data suggest (Khalil and Shearer 1993) that animal husbandry and rice cultivation may have significantly contributed to the rapid growth in emissions of CH_4 observed between 1950–1980. It is interesting to further note that the population of cattle and acreage devoted to rice have been relatively constant over the past several decades: this suggests that the decrease in the growth rate of CH_4 observed in recent years may be attributed at least in part to a slowdown in the growth of the cattle population and in acreage devoted to rice cultivation.

It is clearly important to understand the social and economic factors responsible for the pattern displayed in Figure 17.18. Are the recent trends in cattle population and rice cultivation aberrations resulting in a temporary pause in the growth of emissions of CH_4 or alternately, may they be taken as an indication that sources of CH_4 may have reached an asymptotic limit? The slowdown in the growth of rice acreage may reflect a fundamental limitation imposed by the availability of suitable land; the trend observed in cattle population is more puzzling. A regional analysis could be instructive in elucidating the underlying cause.

Measurements of the ^{14}C content of atmospheric CH_4 suggest that fossil sources account for about 16% of the total contemporary source of atmospheric CH_4.[13] The fossil contribution includes releases from geologic deposits associated with mining of fossil fuels (coal, oil, and natural gas), emissions due to incomplete flaring of gas by the oil industry, and inadvertent losses due to leaks in natural gas pipelines. Contributions from the individual fossil sources are uncertain, and it is difficult to define the temporal trend in associated emissions. It is clear, though, that fossil sources of CH_4 are important and that they may become increasingly significant in the future, reflecting both growth in demand for fossil fuels generally and growth in demand for natural gas specifically. Given the significance of CH_4 as a greenhouse gas, it is important that steps be implemented to eliminate unnecessary, energy-related emissions of CH_4 to the atmosphere.

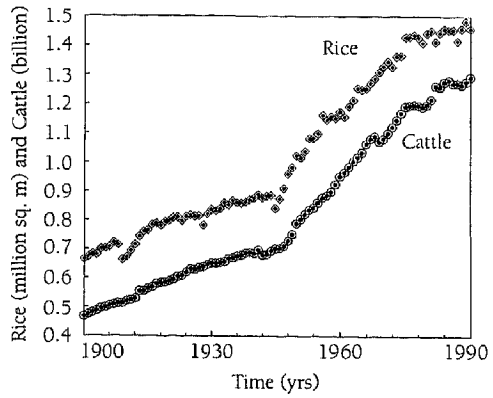

Figure 17.18 Trends in cattle population and rice cultivation over time.

Biomass burning provides an isotopically distinct source of atmospheric CH_4. In contrast to bacterially mediated sources, which tend to favor production of isotopically light carbon (concentrations of $^{12}CH_4$ much larger than $^{13}CH_4$), biomass burning results in the production of CH_4 with isotopic composition comparable to that of the parent fuel. The biomass-burning source has been characterized by a value for $\delta^{13}C$ of about –25‰, typical of C3 plant material (Stevens and Engelkemeir 1988; Wahlen et al. 1989).[14] Bacterial sources, including wetlands, rice cultivation, landfills, and ruminants, exhibit an average value for $\delta^{13}C$ of about –55‰, with a range from about –45 to –70‰ (Quay et al. 1991). The $\delta^{13}C$ of fossil CH_4 is reported as intermediate between that for bacterial production and biomass burning, about –37‰, with a range from as low as –76 to as high as –15‰ (Quay et al. 1991).

Measurements of the isotopic composition of CH_4 trapped in polar ice suggest that $\delta^{13}C$ for atmospheric CH_4 has increased by about 2‰ over the past several decades. The value of $\delta^{13}C$ for CH_4 satisfies an equation of the form

$$\frac{d(N\delta)}{dt} = \sum_i p_i \delta_i^s - N\nu(\delta - \theta), \tag{17.93}$$

where N defines the abundance of CH_4 in the atmosphere (expressed in Tg), δ is the value of $\delta^{13}C$ for atmospheric CH_4 (given in ‰), p_i denotes the rate for production associated with source i (Tg yr^{-1}), δ_i^s (‰) is the value for $\delta^{13}C$ corresponding to source i, ν is the loss frequency (the inverse of the CH_4 lifetime expressed in yr^{-1}), and θ (‰) allows for the selective removal of $^{12}CH_4$ relative to $^{13}CH_4$.

The abundance, N, is given by

$$\frac{dN}{dt} = \sum_i p_i - N\nu \tag{17.94}$$

In steady state, the time derivatives on the left-hand side of (17.93) and (17.94) vanish. In this case,

$$N\nu(\delta - \theta) = \sum_i p_i \delta_i^s \tag{17.95}$$

and

$$N = \nu^{-1} \sum_i p_i = \nu^{-1} p, \tag{17.96}$$

where p denotes the combined source associated with the individual contributions p_i. Combining (17.95) and (17.96), it follows that

$$(\delta - \theta) = \frac{1}{p} \sum_i p_i \delta_i^s \tag{17.97}$$

Under circumstances where either or both of N and δ are observed to vary with time, the derivative on the left-hand side of (17.93) may be expanded and may be rewritten in the form

$$N\frac{d\delta}{dt}+\delta\frac{dN}{dt}=\sum_i p_i\delta_i^s-Nv(\delta-\theta) \qquad (17.98)$$

Equation (17.98) may be employed to estimate the production-weighted average value of $\delta^{13}C$ defining the source of CH_4, using data (from observations, for example) for $d\delta/dt$ and dN/dt and assuming appropriate values for N, v, and θ.

In steady state, the isotopic composition of atmospheric CH_4 is determined by the production-weighted average isotopic composition of the source, corrected to allow for differential removal of $^{12}CH_4$ relative to $^{13}CH_4$.

A budget for atmospheric CH_4, constrained to be consistent not only with information on rates for production by individual sources but also with isotopic data for specific sources, is presented in Table 17.9. The Table distinguishes between sources for the preindustrial environment and more recent contributions associated with the diverse forms of human activity outlined above. The following examples illustrate that the change in $\delta^{13}C$ implied by the data in Table 17.9 is consistent with the trend inferred from analysis of the ice core data. Rows 1–2 refer to the preindustrial environment. Rows 3–7 summarize data attributed to various forms of human activity in the contemporary environment.

Example 17.24: Using the data from Table 17.9, estimate the average value, $\overline{\delta^s}$, for $\delta^{13}C$ associated with preindustrial sources of CH_4.

Answer:

$$\sum_{i=1}^{2} p_i\delta_i^s=-12{,}500$$

$$\sum_{i=1}^{2} p_i=230$$

$$\overline{\delta^s}=-54.3‰ \quad \blacksquare$$

Example 17.25: Using the data in Table 17.9, assuming steady state, estimate the average value, $\overline{\delta^s}$, for $\delta^{13}C$ associated with contemporary sources of CH_4.

Answer:

$$\sum_{i=1}^{7} p_i\delta_i^s=-30{,}820$$

$$\sum_{i=1}^{7} p_i=590$$

$$\overline{\delta^s}=-52.2‰ \quad \blacksquare$$

The last column of Table 17.9 presents values for production attributed to individual sources of CH_4, weighted by the difference between $\delta^{13}C$ for individual sources combined with the average value of $\delta^{13}C$ for the composite source, as estimated in Example 17.25 for the contemporary environment. Positive values of $p_i(\delta_i^s-\overline{\delta^s})$ indicate sources that tend to raise the average value of $\delta^{13}C$ (δ) for CH_4 in the atmosphere. Negative values highlight sources that contribute to a reduction in δ. According to these data, energy-related emissions are primarily responsible for the recent increase in δ for atmospheric CH_4, with a significant additional contribution from biomass burning. The tendency for energy-related emissions and biomass burning to raise the average value of δ for atmospheric CH_4 is partially offset by emissions of isotopically light CH_4 contributed by cattle and rice cultivation.

As indicated above, the rate of increase of atmospheric CH_4 has significantly slowed over the past few decades. The key question is whether this can be taken as a guide for the future: has the concentration of atmospheric CH_4 reached an asymptotic limit or is the rapid rate of increase observed prior to 1980 likely to resume, or even reverse sign, in the future? It seems unlikely that the behavior observed in the most recent period can be taken as a reliable guide for the future.

Table 17.9 Rates for Production and Isotopic Data for Specific Sources of CH_4.

Source	Production, p_i (Tg CH_4 yr^{-1})	δ_i^s (‰)	$p_i\delta_i^s$ (Tg CH_4‰ yr^{-1})	$p_i(\delta_i^s-\overline{\delta^s})$ (Tg CH_4‰ yr^{-1})
1 Wetlands	225	−55	−12,375	−630
2 Biomass burning	5	−25	−125	+136
3 Energy	95	−37	−3515	+1444
4 Landfills	40	−51	−2040	+48
5 Ruminants	80	−62	−4960	−784
6 Biomass burning	35	−25	−875	+952
7 Rice	110	−63	−6930	−1188

Warming at high latitudes could contribute to an increase in the prevalence of stagnant pools of water overlying reservoirs of organic-rich soils. This could give rise to an increase in what might be otherwise considered a natural source of CH_4 (except, of course, that the warming may arise as a consequence of human-induced changes in the concentration of greenhouse gases). Similarly, changes in climate in the tropics favoring warmer and wetter conditions could also result in an increase in emissions. As noted in our discussion of climates of the past, it is clear that natural sources of CH_4 can respond rapidly to regional changes in climate. If steps are to be taken to offset possible climate-related increases in emissions of CH_4, it is essential that we act to reduce, where possible, sources of CH_4 for which we must assume primary responsibility: notably, emissions related to cattle, rice, energy production, biomass burning, and waste disposal. Changes in dietary preferences for meat products, justified on health grounds, could reduce demands for cattle and other ruminants. Selection of strains of rice minimizing emissions of CH_4 to the atmosphere could reduce the rice-related source: CH_4 is transferred from sediments of rice paddy fields mainly through stems of plants, rather than directly through the water column. Steps could be taken to minimize losses of CH_4 associated with unnecessary leaks in pipelines and to capture CH_4 released as a by-product of oil, gas, and coal production. Unnecessary burning of biomass could be eliminated and CH_4 produced by decomposition of organic waste could be captured and used as a substitute for alternative primary fuels.

17.8 Summary

The hydroxyl radical, as we have seen, plays a critical role in tropospheric chemistry: it is responsible for removal of a variety of chemically reduced gases, including CO, CH_4, and a host of hydrocarbons of both natural and anthropogenic origin; it is produced by reaction of $O(^1D)$ with H_2O, with $O(^1D)$ formed by photodissociation of O_3. Production of $O(^1D)$ takes place over a narrow range of wavelengths between about 300 and 310 nm, limited on the long-wavelength limit by the rapid drop-off of the cross section for dissociation of O_3 and limited on the short-wavelength side by the even more rapid decrease in the flux of solar radiation penetrating to the troposphere through the thick protective overlying layer of stratospheric O_3. Not surprisingly, the concentration of OH and the oxidative capacity of the troposphere were found to sensitively depend not only on the abundance of O_3 in the troposphere but also on the height-integrated density of O_3 in the stratosphere.

Ozone is supplied to the troposphere in part by transport from the stratosphere, in part by in situ chemical production. Production in situ occurs as a by-product of the oxidation of reduced gases, such as CO and CH_4. It is catalyzed by reactions involving hydrogen and nitrogen radicals. Three distinct chemical regimes were identified. When the abundance of NO_x is extremely low, oxidation of reduced species results in net *loss* of tropospheric O_3. If the abundance of NO_x is high enough to ensure that peroxy radicals such as HO_2 react with NO, rather than with O_3, oxidation of hydrocarbons and CO is expected to result in net production of O_3. If hydrogen radicals are removed primarily through formation of H_2O_2, the rate for production of O_3 is proportional to the abundance of NO_x. This defines an environment we identified as *NO_x limited.* When concentrations of NO_x are very high, such that hydrogen radicals are removed mainly by formation of HNO_3, the rate for production of O_3 is proportional to the abundance of hydrocarbons. We referred to this regime as *hydrocarbon limited.*

On a global scale, the abundance of O_3 in the troposphere at the present time primarily reflects a balance between in situ chemical production and loss: supply from the stratosphere is small by comparison. On average, the troposphere appears to be NO_x limited, although hydrocarbon limitation may apply in environments where NO_x levels are unusually high (in heavily polluted cities, for example). It is likely that the troposphere was also NO_x limited in the preindustrial environment. The yield of O_3 per NO_x molecule (the number of O_3 molecules produced per molecule of NO_x) varies inversely with respect to the magnitude of the source of NO_x. Production of O_3 is rapid in regions where the abundance of NO_x is high. A large rate for production of O_3 under high-NO_x conditions is compensated by a slower rate for production in regions where concentrations of NO_x are low. Ultimately, globally integrated production of O_3 in the troposphere depends on the rate at which hydrocarbons and CO are made available for oxidation.

The globally averaged abundance of tropospheric OH should be relatively constant in time. This was attributed to the fact that the concentration of OH should vary approximately as $S_n/S_c^{3/2}$ under NO_x-limited conditions, where S_c and S_n define the magnitudes of the sources for hydrocarbons and NO_x, respectively. A change in emission of hydrocarbons may be compensated by a change of similar sign in emissions of NO_x. Adopting the lifetime of CH_4 inferred for the contemporary environment, we used this result in combination with concentrations of CH_4 inferred from studies of gases trapped in ice cores to reconstruct the history of CH_4 emissions over the past 250 years. The rapid growth in emissions in the post–World War II period was attributed primarily to increases in the population of domestic ruminants and in acreage devoted to rice cultivation. The growth in emission of CH_4 has significantly slowed over the past few decades. We suggest, however, that this should not be taken as a reliable guide for the future; a warmer and wetter climate may result in an increase in emissions from natural sources: wetlands, for example. To offset possible increases in emissions from natural sources, steps should be taken to reduce emissions from sources associated more directly with human activity: ruminants, rice cultivation, fossil fuel industry, biomass burning, and waste disposal.